NOVEL TECHNIQUES OF ARRAY ANTENNA DESIGN FOR SATELLITE COMMUNICATION

Ph.D. THESIS

Javad JANGI GOLEZANI

Department of Communication Systems

Satellite Communication and Remote Sensing Programme

FEBRUARY 2017

ISTANBUL TECHNICAL UNIVERSITY ★ INFORMATICS INSTITUTE

NOVEL TECHNIQUES OF ARRAY ANTENNA DESIGN FOR SATELLITE
COMMUNICATION

Ph.D. THESIS

Javad JANGI GOLEZANI
(705122002)

Department of Communication Systems

Satellite Communication and Remote Sensing Programme

Thesis Advisor: Prof. Dr. Selçuk PAKER

FEBRUARY 2017

İSTANBUL TEKNİK ÜNİVERSİTESİ ★ BİLİŞİM ENSTİTÜSÜ

UYDU HABERLEŞMESİ İÇİN YENİ DİZİ ANTEN TASARIM YÖNTEMLERİ

DOKTORA TEZİ

Javad JANGI GOLEZANI
(705122002)

İletişim Sistemleri Anabilim Dalı

Uydu Haberleşmesi ve Uzaktan Algılama Programı

Tez Danışmanı: Prof. Dr. Selçuk PAKER

ŞUBAT 2017

Javad-jangi golezani, a Ph.D. student of İTU Informatics Institute student ID 705122002, successfully defended the thesis entitled "NOVEL TECHNIQUES OF ARRAY ANTENNA DESIGN FOR SATELLITE COMMUNICATION", which he prepared after fulfilling the requirements specified in the associated legislations, before the jury whose signatures are below.

Thesis Advisor :   **Prof. Dr. Selçuk PAKER**   ....
ISTANBUL Technical University

Jury Members :   **Assoc. Prof. Dr. Mesut KARTAL**   ....
ISTANBUL Technical University

Assoc. Prof. Dr. Cevdet IŞIK   ....
ISTANBUL Technical University
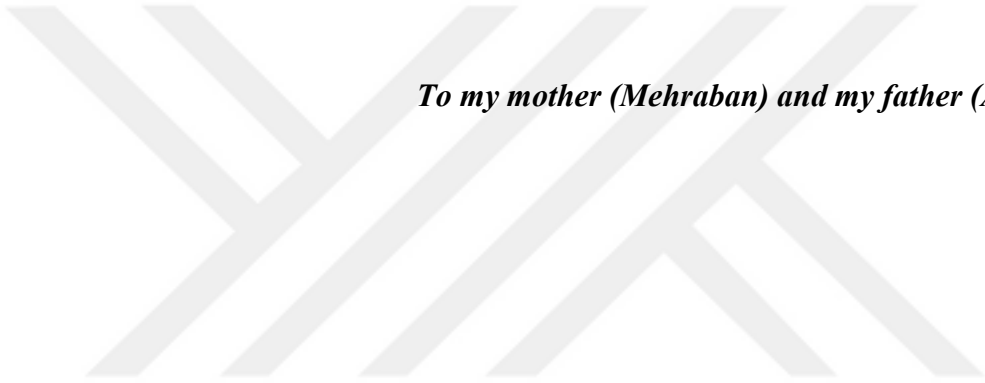
Prof. Dr. Ahmet KIZILAY   ....
Yıldız Technical University

Assist. Prof. Dr. Aktül KAVAS   ....
Yıldız Technical University

Date of Submission : 30 December 2016
Date of Defense   : 13 February 2017

To my mother (Mehraban) and my father (Allahvirdi),

FOREWORD

I would like to express my deepest gratitude to my advisor Prof. Dr. Selçuk PAKER for his continuous support of my PhD work. Completion of this PhD thesis was possible with his guidance and insightful ideas that have enriched my study. Also, I received all the helps that I needed to access to the facilities and services in the University or everywhere in all steps to fulfil my work. Thank you for offering all the supports and also for your endless motivation during my study in Istanbul Technical University.

My sincere thanks also goes to Assoc. Prof. Dr. Mesut KARTAL. I appreciate his supports during my study in Istanbul Technical University. He was also a member of my thesis supervisory committee offering constructive suggestions during my research.

I would like also to appreciate Assist. Prof. Dr. Aktül KAVAS for taking the time to be on my thesis supervisory committee. She has been offering helpful suggestions which improved my work. Besides her, my special thanks to the rest of my thesis jury committee Assoc. Prof. Dr. Cevdet IŞIK and Prof. Dr. Ahmet KIZILAY for their insightful suggestions which enriched my thesis.

I must express my gratitude to Prof. Dr. Constantine A. BALANIS from Arizona State University to take his precious time to contribute to our research work. I feel extremely honored and appreciative for receiving his significant contribution.

No research is possible without laboratory work and services. I appreciate RF Laboratory group of the Electric and Electronics Engineering Faculty of İTÜ and particularly Dr. Bülent YAĞCI for all the services and facilities that made me opportunity to do my work. Also, very thanks to PROFEN Group Company for their contribution in measurement process. My thanks to all my friends in Istanbul and Istanbul Technical University who supported me in every possible way.

Foremost, I would like to thank to my beloved Parents who encouraged and helped me at every stage of my personal and academic life. I am forever indebted to my mother (Mehraban), my father (Allahvirdi), my sister (Masi) and my brother (Reza) for their understanding, endless patience and encouragement when it was most required. Thank you for your boundless love encouraging and supporting me both physically and morally in difficulties. You are my life's angels, I dedicate this work to you as you are my invaluable precious persons in the world.

February 2017   Javad JANGI GOLEZANI

TABLE OF CONTENTS

ABBREVIATIONS

AF	**:** Array Factor
AUT	**:** Antenna Under Test
CCAA	**:** Concentric Circular Antenna Array
DGS	**:** Defected Ground Structure
DMS	**:** Defected Microstrip Structure
GA	**:** Genetic Algorithm
HFSS	**:** High Frequency Structure Simulator
HPBW	**:** Half Power Beam Width
ITU	**:** International Telecommunication Union
RCGA	**:** Real Coded Genetic Algorithm
SIW	**:** Substrate Integrated Waveguide
SLL	**:** Side Lobe Level

LIST OF TABLES

LIST OF FIGURES

NOVEL TECHNIQUES OF ARRAY ANTENNA DESIGN FOR SATELLITE COMMUNICATION

SUMMARY

Antennas with high directivity or narrow beam width are preferred to be used in satellite communications to offer better reception performance in terms of reducing interferences from dense geo orbital sources. Sources of interference mostly are nearby satellites, other nearby earth stations or nearby microwave towers. Consequently, array antennas with high number of elements are developed over the past decades to obtain high directivity, narrow beam width and low side lobe level to minimize interference from these unwanted sources.

On the other hand, increasing number of the elements in the design of arrays causes to long microstrip lines in feed network leading to dielectric and ohmic losses. Also, the use of large number of power splitters leads to increasing insertion and isolation losses. The power-splitting network is also limiting the band width and enlarging the size. Therefore, optimization of feed network of large arrays has been investigated extensively. Moreover, miniaturizing the dimensions of antenna used in both satellite or ground station have been subject of developed studies. Consequently, main goal of this thesis is to determine methods for array antenna design with higher directivity, low side lobe level, effective feed network and smaller dimensions.

Radiation characteristics of an array depends on the radiation pattern of the element antenna and the geometrical configuration along with relative displacement and excitation of the overall array described by the array factor. Most of the available design techniques are accomplished by optimizing the array factor, neglecting abilities of the element antennas. In Chapter 4 of this thesis, three novel approaches of array design are proposed by using different combinations of special element antennas. In comparison with existing design procedures, the novel proposed methods are based on effective uses of both array factor and element factor with respect to each other. Consequently, array antennas with small aperture, effective feeding or narrow beam width are designed by using three distinct novel methods. Accuracy of all the approaches are confirmed based on theoretical studies and calculations. However, validity of the techniques are also demonstrated with simulations or measurement of prototype antenna(only for section 4.2). All the designs and simulations are accomplished in the range between 10.7GHz and 12.7 GHz which is allocated as satellite downlink for KU band.

In section 4.1 of this thesis, a novel method is proposed to design array antenna with desirable directivity but smaller aperture compared to the method used in available designs. The design approach is well-demonstrated in two-element array structure. In an array with two elements, although reducing the element spacing from λ to $\lambda/2$ causes to a wide beam, but the resulting beam has no side lobs. Consequently, a special element antenna having a beam with a more narrow main lobe and probable side lobs at any other directions can be used to achieve a beam with single narrow lobe. Then,

this approach can be developed to design arrays with large number of elements with small element spacing. Accuracy of the method is demonstrated and studied by using Ansoft HFSS software simulations.

The second novel approach (section 4.2) proposes a method to design a low loss array antenna. It is demonstrated that the same beam width can be achieved by using 2λ element spacing with half the number of elements compared to the design with conversional limit of λ element spacing. Consequently, reducing the number of elements in microstrip arrays leads to lowering the loss made by long feed lines and insertion or isolation loss made by the power splitters. Also, using larger element spacing lowers the coupling between adjacent elements. However, the method needs a directive element antenna to cancel additional lobes. An element antenna with a very directive beam is simulated and fabricated. Then, a prototype array antenna is also simulated and fabricated based on the method with 2λ spacing of that element antenna and the measured results are provided to confirm the method.

Results of section 4.2 confirms that beam width of an array is determined by aperture length of the array; more clearly by the elements placed towards the ends of the array. Subsequent results confirms that those additional interior elements are mostly effective in cancelling minor lobes, while having negligible effect on the beam width. Therefore, placement of the interior elements towards the ends of the array is aimed to improve the beam width, while this method distorts the side lobes. This is considered as a favorite achievement given that in some cases such as satellite applications the beam width of main lobe is more required than the side lobe level. Consequently, a novel nonlinear array design is presented in section 4.3 to achieve a narrower beam width with acceptable side lobe level compared to linear array.

Chapter 5 of this thesis presents the forth study on array antennas advantageous for the satellite communication applications. Although, the methods in Chapter 4 confirm the good results in terms of small dimensions, efficiency and beam width. However, quality of a directive antenna in suppressing the interferences is described by its side lobe level. Regarding that the most favorite approach for this aim is the Binomial array, study of Binomial arrays is presented in Chapter 5.

Binomial arrays, favorably show low side lobe level due to smooth amplitude distribution from the center element toward those at the edges. As the other advantage, binomial arrays with the element spacing equal or less than $\lambda/2$ have no minor lobes. However, unfortunately, there are no compact expressions for the array factor and directivity for binomial arrays with no restriction in element spacing, except for $\lambda/2$ spacing. In chapter 5, a novel procedure is proposed to derive compact expressions for the array factor and directivity of binomial arrays. The properties of Pascal's triangle, upon which the excitation coefficients of the binomial array are based and distributed, are used to obtain the compact expressions. It is demonstrated that the excitation coefficients of an N-element binomial array can be expressed as an (N-2)th convolution of the two-element binomial array. Then, the array factor and directivity of the entire binomial array is obtained using the properties of Fourier transform.

UYDU HABERLEŞMESİ İÇİN YENİ DİZİ ANTEN TASARIM YÖNTEMLERİ

ÖZET

Sıkışık geo orbital kaynaklardan gelen girişimlerin azaltılması açısından daha iyi alım performansı sunmak için yüksek yönlendiricili veya dar demete sahip antenlerin kullanılması uydu haberleşmesinde tercih edilir. Girişim kaynakları genelde yakın uydular, yakın diğer yer istasyonları veya yakındaki mikrodalga kuleleri olabilirler. Sonuç olarak, bu istenmeyen kaynaklardan gelen bozucu girişimleri en az seviyeye indirmek amacı ile yüksek yönlendiricilik, dar demet ve düşük yan lob seviyesi elde etmek için son on yıllar boyunca yüksek sayıda eleman içeren dizi anten çözümleri geliştirilmiştir.

Ancak, çok tercih edilen mikroşerit antenlerde, uzun mikro şerit hatların kullanımı, çok sayıda eleman içeren dizilerin tasarımında neredeyse imkansız kılmaktadır. Öte yandan, güç paylaşım devrelerindeki çok sayıda güç ayırıcının kullanılması izolasyon kaybının artmasına, bant genişliğinin sınırlandırılmasına ve boyutun büyümesine neden olmaktadır. Bu nedenle, besleme devresinin iyileştirilmesi, kısaltılmış şerit hatlarına sahip olmak için veya güç bölücülerin sayısını düşürmek için yeni bir çözüme ihtiyaç duyulmaktadır. Seri beslenen ağ sistemi, tüm tasarımlarda ideal bir yöntem olmamasına rağmen, güç ayırıcıların sayısını ve iletim hatlarının uzunluğunu azaltmak için önerilen yöntemlerden biridir. Diğer yöntemler arasında, maliyet etkin olmayan, aynı zamanda dizi anteninin boyutunda genişlemeye yol açan ama besleme ağı kaybını azaltan kılavuzlarının kullanımı da bulunmaktadır. Tabana entegre olmuş dalga kılavuz yaklaşımı, aynı zamanda küçük boyutlara sahipken, kayıpları azaltmada etkili bir yöntem olarak önerilmektedir. Ama, yine de uygun maliyetli bir yöntem değildir.

Dar demetli yönlü antenlerin yanı sıra, girişimlerin üstesinden gelmek için sadece yan lob seviyesini optimize eden tekniklerde önerilmiştir. Bazı tasarımlarda yan lob seviyesini azaltmak için, elemanlar arası eşit olmayan aralık kullanımı önerilmektedir. Simetrik dairesel anten dizisi (CCAA) ve eşit aralıklı olmayan küresel diziler de, yan lob seviyesi küçültülmektedir. Optimize edilmiş dizi tanımlamak için ayrı incelemlerde yapılmaktadır. Genetik Algoritmalar (GA) gibi algoritmalarda, yan lob seviyesinin bastırmasına yol açan etkili yöntemler olarak önerilmiştir. Ancak, bu tasarımlardan bazıları yan lob seviyesinde sınırlı bir iyileştirmeye neden olabilmektedirler. Buna ek olarak, bazı yöntemler, istenilen yan lob seviyesini sınırlı sayıda elemanlı diziler için önerilmiştir. Gerçek Kodlamalı Genetik Algoritma (RCGA) kullanan diğer yöntemler ise, standart diziden daha büyük bir dizi boyutuyla sonuçlanmakta ve bu da dezavantaj olarak değerlendirilmektedir.

Antenin boyutları da fazla sayıda araştırmaların ve çalışmaların konusu olmuştur. Şekillenmiş mikro şerit yapılı (DMS) veya şekillenmiş toprak yapılı (DGS) yöntemlerin kullanılması önerilmiştir. Ancak, bu tasarımlar verimliliğin düşmesine neden olmaktadır. E-şekilli bir DGS dizi anten, boyutları küçülmüş, ancak optimum verimliliğe sahip olması için önerilmektedir. Buna rağmen yüksek sayıda olan dizilerde arzu edilen bir yöntem olmamaktadır. Diğer tekniklerden bir örnek olarak,

uydu uygulamaları için yapay manyetik malzemeler kullanarak minyatür dizi anten çözümleri önerilmektedir. Fakat maliyet açısından etkili bir yöntem değildirler.

Sonuç olarak, bu tezin ana amacı, daha pratik ve az maliyetli yüksek yöneltilebilirlik, düşük yan lob seviyesi, etkili besleme ağı ve daha küçük boyutlara sahip olan yeni dizi anten tasarım yöntemlerini belirlemektir. Bir dizinin ışıma karakteristikleri, eleman anteninin ışıma modeline ve dizilim faktörü olarak tanımlanmış olan dizi geometri konfigürasyon, toplam dizinin nispi yer değişimi ve beslenme devresine bağlıdır. Mevcut tasarım tekniklerinin çoğu, eleman antenlerin kabiliyetini ihmal edip dizi faktörünü optimize ederek gerçekleştirilir. Bu tezin 4. bölümünde, özel eleman antenlerinin farklı kombinasyonları kullanılarak dizi tasarımında üç yeni yaklaşım önerilmiştir. Mevcut tasarım yöntemleri ile karşılaştığında, yeni önerilen yöntemler, hem dizi faktörünün hem de eleman faktörünün ikisinde birbirine göre etkin kullanımlarına dayanmaktadır. Sonuç olarak, küçük açıklıklı, az kayıplı besleme veya dar demetli dizi antenleri üç farklı yeni yöntem kullanılarak tasarlanmıştır. Bu nedenle, dalga kılavuzu beslemeli diziler gibi diğer tasarımlarla karşılaştırıldığında, önerilen teknikler, imalat maliyetleri ve tasarım basitliği açısından daha pratik bir sonuç vereceği görülmüştür.

Üç farklı önerilen yaklaşım ayrıntılı olarak incelenmiştir. Bütün yaklaşımların doğruluğu teorik hesaplamalara dayanarak teyit edilmiştir. Teorik çalışmaların yanı sıra, Ansoft HFSS simülasyonları kullanılarak birinci yaklaşımın (bölüm 4.1) ve üçüncü yaklaşımın (bölüm 4.3) sonuçları gösterilmiştir. Bununla birlikte, Bölüm 4.2'de sunulan yönteme dayanarak bir anten dizisi üretilmiştir. Tezin 5. bölümünde Binom dizilerinin yönlendiricilik parametresini hesaplamak için bir yeni yöntem gösterilmektedir. Önerilen yöntemlerin bir özeti basitçe açıklanmaktadır.

Ku bant uydu teknolojisi, iletişim dünyasında kritik bir rol oynamaktadır. İnternet erişimi ve TV yayıncılığı gibi farklı uygulamalar Ku bant kullanan hizmetlerin örneğidir. Bu tezde önerilen prototip antenler Ku band frekanslarının aşağı bağlantı aralığında kullanılmak üzere doğrusal polarizasyonlu alıcı olarak tasarlanmıştır. Bu araştırmada, Ku band uydu iletişim sistemleri için aşağı bağlantı olarak tahsis edilen 10.7 GHz ila 12.7 GHz (10-18 GHz arasında) aralığı, dikkate alınmıştır.

Bu tezin 4.1 bölümünde, istenilen yönelticilik özelliğine sahip olan ama mevcut tasarımlarda kullanılan yöntemle karşılaştırıldığında, daha küçük açıklık ile dizili anten tasarlamak için yeni bir yöntem önerilmiştir. Bu tasarım yaklaşımı, iki elemanlı dizi yapısında etkin bir şekilde gösterilmiştir. İki elemanlı bir dizide eleman aralığını λ'dan $\lambda/2$'ye indirgemek geniş bir demet açısına neden olurken, ancak ortaya çıkan demetin yan lobları yoktur. Sonuç olarak, tek dar loblu bir demet elde etmek için, daha dar bir ana lob ve herhangi bir başka yönde muhtemel yan lobları olan bir demete sahip olan özel bir eleman anten kullanılabilir. Ardından, bu yaklaşım, küçük eleman aralığıyla çok sayıda eleman içeren dizileri tasarlamak için geliştirilebilir. Yöntemin doğruluğu, Ansoft HFSS yazılım simülasyonları kullanılarak gösterilip ve incelenmiştir.

İkinci yeni yaklaşım (bölüm 4.2), düşük kayıplı bir dizi anten tasarlamak için bir yöntem önermektedir. Aynı demet açısı, geleneksel λ eleman aralığı sınırı ile tasarıma kıyasla eleman sayısının yarısı ile 2λ eleman aralığı kullanılarak elde edilebileceği gösterilmiştir. Sonuç olarak, mikro şerit dizilerindeki eleman sayısının azaltılması, uzun besleme hatları tarafından yapılan kayıpların ve güç bölücülerin izolasyon kaybının azalmasına neden olmaktadır. Ayrıca, daha büyük eleman aralığı kullanılarak komşu elemanlar arasındaki kuplaj etkisi de azalmaktadır. Ancak, yöntemin yarattığı ek lobları kaldırmak için bir yüksek yönlendiricili eleman anteninin kullanımına ihtiyaç duyulmaktadır. İstenilen yüksek yönlendiricili eleman anten için çözüm

önerilerek benzetimi yapılmış ve baskı devre ile elde edilen prototip ölçülerek tasarım ile karşılaştırılmıştır. Ardından, 2λ eleman aralığına sahip olan ve bu yönteme dayanılarak bir prototip dizi anteni simüle edilip ve bastırılmıştır. Yöntemi doğrulamak için prototip antenin ölçülmüş S11 parametresi ve ölçülmüş ışıma karakteristikleri sunulmaktadır.

Bölüm 4.2'deki sonuçlar, bir dizinin demet açısının dizinin açıklık uzunluğu tarafından belirlendiğini teyit etmektedir; dizi demet genişiliği daha net bir şekilde dizinin uçlarına doğru yerleştirilen elemanlarla belirlenmektedir. Sonraki sonuçlar, bu ek iç elemanlar, yan lobların kaldırılması için çoğunlukla etkili olduğunu ve demet açısında ihmal edilebilir bir etkiye sahip olduğunu doğrulamaktadır. Bu nedenle, iç elemanların dizinin uçlarına doğru yerleştirilmesi, demet açısı iyileştirmeyi amaçlarken bu yöntem yan lobları deforme olmasına yol açmaktadır. Uydu haberleşmesi uygulamaları gibi bazı durumlarda ana lobun demet açısı yan lob seviyesinden daha fazla etkili bir parametre olması nedeniyle, bu yöntem en istenilen çözümü oluşturan yeni bir yaklaşım yöntemi oluşturacaktır. Sonuç olarak, doğrusal diziyle karşılaştırıldığında kabul edilebilir yan lob seviyesi ile daha dar bir demet açısı elde etmek için bölüm 4.3'te yeni bir doğrusal olmayan dizi tasarımı sunulmuştur.

Bu tezin 5. bölümünde, uydu iletişimi uygulamaları için avantajlı olan dizi antenleri üzerinde yapılan 4. çalışma sunulmaktadır. Bununla birlikte, Bölüm 4'teki yöntemler küçük boyutlar, verimlilik ve demet açısı açısından iyi sonuçları teyit etmektedir. Ancak, yüksek yönelticilikli bir antenin girişimi bastırma kalitesi yan lob seviyesi ile tanımlanmaktadır. Bu amaca yönelik en uygun yaklaşım Binom dizisi olduğu için Binom dizilerinin incelenmesi Bölüm 5'te sunulmuştur.

Binom dizileri, merkez elemandan kenarlardaki elemanlarına kadar düzgün azalan genlik dağılımına bağlı olarak olumlu şekilde düşük yan lob seviyesini elde edilebileceğini göstermektedir. Diğer avantaj olarak, eleman aralığı $\lambda/2$'ye eşit veya daha küçük olan binom dizileri yan loblara sahip değildirler. Ancak, $\lambda/2$ aralığı haricinde, eleman aralığında herhangi bir kısıtlama olmaksızın, binom dizileri için dizi faktörü ve yönlendiricilik parametresi için kompakt ifadeler mevcut değildir. Bölüm 5'te, binom dizilerinin dizilim faktörü ve yönlendiricilik parametresi için kompakt ifadeler türetmek için yeni bir yöntem önerilmiştir. Binom dizisinin besleme katsayılarının dayandığı ve dağılmış olduğunu gösteren Pascal üçgeninin özellikleri kompakt ifadeleri elde etmek için kullanılmıştır. Bir N elemanlı binom dizisinin besleme katsayılarının, iki elemanlı binom dizisinin bir (N-2) konvolüsyonu olarak ifade edilebileceği gösterilmiştir. Daha sonra, binom dizisinin tümünün dizi faktörü ve yönlendiricilik parametresi, Fourier dönüşümü özelliklerini kullanarak elde edilmiştir.

1. INTRODUCTION

First developments in the world of directive antennas emphasizing their importance in long-range communications are carried out by Marconi [1] at around 1920s. Then, several advances such as phased array technology are accomplished in the field of array antennas. The requirements of World War II emphasized the role of array antennas [1] leading to further development in this field. Nowadays, the concept of smart antennas are arisen. Although, an antenna array may be used in a variety of ways to improve the performance of a communication system, but, the most important one is its capability to suppress interferences made in the systems including multiple channels. Several novel approaches are proposed in this thesis to improve those performances of array antennas.

This thesis is organized as follows. Chapter 2 provides the basics and terminology used in understanding antenna arrays. Chapter 3 discusses the application of array antennas in satellite communication. Chapter 4 introduces three novel methods of array design with small aperture, effective feed and narrow beam. Chapters 5 presents a method for calculating the directivity of Binomial array with no restriction on element spacing, for the first time.

1.1 Purpose of Thesis

One of the main requirements of any satellite communication system is to use a highly directional antenna. In satellite communications, there are always some sources of interference, due to using multiple satellites and terrestrial sources, degrading the performance of both satellite system and base station. Then, directive antennas with very low Side Lobe Level (SLL) are required to be used in order to overcome the interferences from unwanted sources [2,3]. Furthermore, antennas with miniaturized dimension are preferred to be used in both base station and satellite [4]. Main aim of this thesis is to propose novel approaches of array antenna design with improved performance in terms of dimensions, Half Power Beam Width (HPBW) and SLL. The methods are carried out by using arrays with appropriate spacing or weighting of

elements and consequently, adjusting the favored beam pattern of the array, along with using special element antennas.

Ku band satellite technology plays a crucial role in the world of communications. Different applications such as internet access and TV broadcasting are services that are using Ku band. The prototype antennas proposed in this thesis are design with linear polarization as the receiver for use in downlink range of Ku band frequencies. The range between 10.7 GHz and 12.7 GHz (from 10-18 GHz) is allocated as downlink for Ku band satellite communication systems, which is considered in this research.

1.2 Literature Review

Regarding that the directivity of element antennas are limited, arrays with high number of elements are used in satellite communications, same as in available designs in [5]. But, the use of long microstrip lines is almost prohibitive in the design of arrays with large number of elements [6,7]. On the other hand, the use of large number of power splitters leads to increase of insertion or isolation loss in the power-splitting network also limiting the band width and enlarging the size [8,9]. Therefore, it is required to improve the feed network having shortened strip lines or lowered number of power splitters. Serially fed network system is one of the methods proposed to reduce the number of power splitters and length of transmission lines [10] while it is not an ideal method in all designs. Other methods include the use of superstrate [11] or waveguides [12,13] to reduce the loss in feed network, where, are not cost effective methods, also leading to enlargement in the size of the array antenna. Substrate Integrated Waveguide (SIW) approach is also proposed in [14] as an effective method in reducing losses, while also having small size. However, it is not a cost effective method.

Dimensions of the antenna also have been subject of developed studies. The use of Defected Microstrip Structure (DMS) [15] or Defected Ground Structure(DGS) [16] are proposed. However, these designs result in reduced size with decreased efficiency. An E-shaped DGS array antenna is proposed with reduced size but having optimum efficiency, which still is not a desirable method in arrays with large number of elements. The other technique is proposed in [17] proposing miniaturized array antenna using artificial magnetic materials for satellite applications. But, it is not a cost effective method.

Besides the efficiency and size, in many of the practical applications, such as in radar, imaging or satellite communications, it is required to reduce the SLL of the radiation pattern of an antenna array [18,19] to minimize interference from unwanted sources [20]. Several designs have been proposed to reduce the SLL of array antennas. In [21], the use of unequal spacing is proposed to reduce the SLL. A Concentric Circular Antenna Array (CCAA) [22] and unequal spacing in spherical arrays [23] were examined to identify an optimized array with minimized SLL. Metaheuristic algorithms, such as Genetic Algorithms (GA) [24-26] have been proposed as effective methods leading to the SLL suppression. However, some of those designs lead to a limited level of improvement in SLL. In addition, the desired SLL can be obtained for arrays with limited number of elements by using some methods, such as the element placement based on GA [19,24]. In [25], position perturbation of the array elements results in a reduction in the SLL at the central part but with higher minor lobes at the outer parts of the pattern. Other methods such as in [26], using Real Coded Genetic Algorithm (RCGA), result in a larger array size than the original, which may be considered a drawback.

1.3 Hypothesis

In this thesis, three novel distinct methods are proposed to design array antennas with smaller aperture, effective feeding and narrower beam compared to the existing design methods. The proposed methods are based on effective use of array factor along with special element antennas. Therefore, in comparison with other designs such as waveguide-fed arrays, the proposed techniques result in more practical performance in terms of simplicity of design and fabrication costs. Three proposed approaches are studied in detail. Beside the theoretical studies, results of the first approach (section 4.1) and the third approach (section 4.3) are demonstrated by using Ansoft HFSS simulations. However, an antenna array is fabricated based on the method presented in section 4.2. Chapter 5 of the thesis also demonstrates a method to calculate the directivity of Binomial arrays. The proposed methods are simply clarified in this section.

In the first approach (section 4.1), a novel array antenna with desired directivity but smaller aperture compared to available designs is presented. It is a well-established fact that directivity of arrays increase by increase of the aperture dimensions [27,28].

However, a design with high directivity is introduced by using a reduced element spacing compared to the conventional design. This method is based on the use of a special element antenna with its corresponding array factor.

In the second approach (section 4.2), an array structure with reduced number of elements is proposed. In fact reducing the number of elements leads to lowering the ohmic loss made by long strip lines [6,7]. Its most favorite advantage is low insertion or isolation loss made by reducing the number of power-splitting networks. This can be accomplished by using 2λ element spacing in comparison with λ spacing (used in all available designs). HPBW in both methods does not changes by far where the minor lobes are canceled by using a directional element antenna.

In the third approach (section 4.3), study of a nonlinear array to achieve a narrower beam with acceptable SLL is presented. In fact, HPBW of an array is determined by the aperture length of the array [27]. Therefore, it is aimed to change the position of interior elements towards the ends of the array in a nonlinear form to improve the HPBW.

In chapter 5 of the thesis Binomial arrays are studied as the favorite design in term of SLL. Except for the element spacing of $\lambda/2$, there are no compact expressions for the array factor and directivity for binomial arrays with no restriction in element spacing [27]. In this chapter, compact expressions for the array factor and directivity of binomial arrays are calculated. The properties of Pascal's triangle is used to show that the excitation coefficients of an N-element binomial array can be expressed as an (N-2)th convolution of the two-element binomial array. Then, the array factor and directivity of the entire binomial array is obtained using the properties of Fourier transform.

2. ARCHITECTURE, ADVANTAGES AND APPLICATIONS OF ARRAY ANTENNAS

2.1 Introduction

It was the most significant achievements in early radio communication science when Guglielmo Marconi successfully received the first transatlantic radio message, including the Morse-code for the letter 'S' by three short clicks on December 12, 1901 [1,29]. This communication system and the following improvements emphasized the role of antennas in the world of long range communications. Design and enhancing antenna directivity in order to establish long-range communication has been subject of extensive researches since Marconi published the paper entitled "Directive Antenna" [1,29]. As the milestone era in the world of communication, Karl Ferdinand Braun performed a developed research in directive wireless communication technology. Then, he won the Nobel Prize for demonstrating enhanced transmission of radio waves in one direction [1,30]. As another instance, Beverage invented so-called wave antenna or Beverage antenna with improved gain compared to dipoles and other simple elements [31]. Then, several directive array antennas had been developed by mid 1930s [32], when the directivity of single element is limited. Antennas with fixed beam radiation properties were primarily used to meet the demands for high directivity applications up to 1920s. But, application of array antenna is developed in the next years and demands for arrays with additional operations are increased. As the second milestone era, in 1940s in the second World War the concept of an antenna array was first introduced in military applications in the [1,30]. The progress in the array technology in this era also enabled the antenna system to be electronically steered. In the next years, developments in the field of signal processing led to new progresses in array design [1]. Arrays could be used to receive signals from a particular direction while rejecting signals in unwanted directions. Consequently, arrays could be used to mitigate intentional interference (jamming) or unintentional interference (radiation from other sources) directed toward the communication system by using signal processing algorithms. Development in array technology was continued and the

concept of adaptive antenna arrays is arisen by the further development in signal processing. This improvement again significantly contributed to the capacity available in wireless communication systems. According to these developments, there has been a large amount of work on algorithms and the signal processing aspects in early array technology. But unfortunately, the physical geometry (or location of the antenna elements in the array) has received relatively little attention.

2.2 Array Principle and Architecture

Total electrical field of an array of identical elements is demonstrated by multiplication of the radiation pattern of a single element and the array factor [27], as in (2.1).

$$\vec{E}(total) = \left[\vec{E}\ (single\ element)\right].[array\ factor] \tag{2.1}$$

where, $\vec{E}$ demonstrates vector electric field.

The array factor, is a scalar function of the number of elements, their geometrical positioning, their relative magnitudes, their relative phases and their spacing's. The array factor for all the arrays in this thesis is calculated independent of the polarization of the elements and coupling between the elements (it is assumed that all the elements have same polarization and coupling between the elements is negligible). As the array factor is independent of the directional characteristics of the radiating elements, then it can be formulated by replacing the actual elements with equally polarized isotropic (point) sources. Therefore, for the two-element (point sources) array with identical excitation in Figure 2.1, the normalized array factor is presented in (2.2) [27].
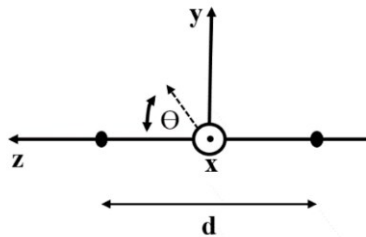
Figure 2.1 : Array of two elements along the Z axis.

$$AF = \frac{e^{+j\psi/2} + e^{-j\psi/2}}{2} \tag{2.2}$$

where,

$$\psi = kd \cos \theta + \beta \tag{2.2a}$$

where, β is the difference in phase excitation between the elements, $k \left(\frac{2\pi}{\lambda}\right)$ is wave constant, d is the spacing between the elements and the angle θ is demonstrated in Figure 2.1.

Then, consider an array with N elements each placed with d spacing relative to each other, where the first element place in $z = 0$. Assuming that the elements have identical excitation coefficients but β progressive phase relative to each other, the normalized array factor is given by (2.3) [27].

$$AF = \sum_{n=1}^{N} e^{j(n-1)\psi} \tag{2.3}$$

The normalized array factor in (2.3) can also be expressed in more compact form by shifting reference point to center of array as in (2.4) [27].

$$AF_n = \frac{1}{N} \left[\frac{\sin\left(\frac{N}{2}\psi\right)}{\sin\left(\frac{1}{2}\psi\right)} \right] \tag{2.4}$$

In addition to linear arrays, the elements can be positioned in rectangular or circular forms as planar arrays. Planar arrays provide additional variables which can be used to control and shape the pattern and could provide more symmetrical patterns with lower side lobes. Consider Figure 2.2a in which M elements are positioned along the x axis as a linear array.
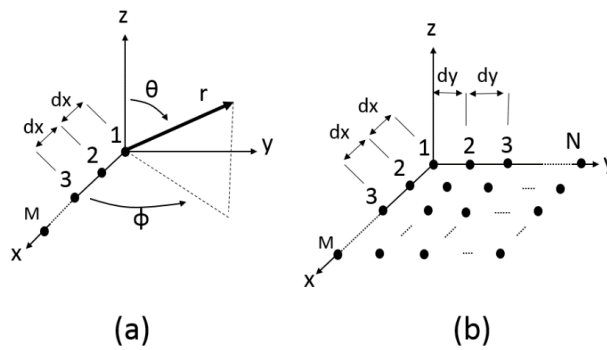
Figure 2.2 : (a) Linear array (b) Planar array.

The planar array demonstrated in Figure 2.2b would be formed by convolving the linear array in Figure 2.2a with another N-element array along the y axis.

The array factor for the M-element and N-element arrays in x and y axis's respectively, are given by (2.5a) and (2.5b) [27].

$$\text{AF}_{xm} = \sum_{m=1}^{M} I_{m1} e^{j(m-1)(kd_x \sin\theta \cos\phi + \beta_x)} \tag{2.5a}$$

$$\text{AF}_{yn} = \sum_{n=1}^{N} I_{n1} e^{j(n-1)(kd_y \sin\theta \sin\phi + \beta_y)} \tag{2.5b}$$

Where, I_{m1} and I_{n1} are the excitation coefficient of each element in linear arrays along the x and y axis's, respectively. The spacing's between the elements along the x and y axis's are demonstrated by d_x and d_y, respectively. β_x and β_y demonstrate the progressive phase shifts for the linear arrays along the x and y axis's, respectively. Since the planar array in Figure 2.2b can be expressed as the convolution of the two linear arrays, consequently, the array factor for the entire planar array can be written in multiplication form as (2.6) [27].

$$AF = I_0 \sum_{m=1}^{M} e^{j(m-1)(kd_x \sin\theta \cos\phi + \beta_x)} \sum_{n=1}^{N} e^{j(n-1)(kd_y \sin\theta \sin\phi + \beta_y)} \tag{2.6}$$

where, $I_{mn} = I_0$ exhibits the amplitude excitation of any element throughout the array. The compact and normalized form of array factor can also be written as (2.7).

$$AF_n(\theta, \phi) = \left[\frac{1}{M} \frac{\sin\left(\frac{M}{2}\psi_x\right)}{\sin\left(\frac{\psi_x}{2}\right)}\right] \left[\frac{1}{N} \frac{\sin\left(\frac{N}{2}\psi_y\right)}{\sin\left(\frac{\psi_y}{2}\right)}\right] \tag{2.7}$$

where,

$$\psi_x = kd_x \sin\theta \cos\phi + \beta_x \tag{2.7a}$$

$$\psi_y = kd_{xy} \sin\theta \sin\phi + \beta_y \tag{2.7b}$$

Directivity of a linear array increases, relative to a single element, in the plane perpendicular to and containing the linear array antenna. However, the directivity does not change and remains that of a single element in the plane perpendicular to this plane. But, by the positioning the elements in a planar array the directivity would increase in both principal planes of the array antenna.

2.3 Advantages of Array Antennas

An array antenna may be used in a variety of ways to improve the performance of a communication system. The most important is its capability to suppress interferences made in the systems such as satellite communication in both transmit or receive modes. By combining signals from different antennas and consequently, adjusting the beam pattern of the array, it is possible to cancel the interference.

Performance of the array antennas are then developed by using some algorithms combining multiple antennas which are called as phased arrays. The most advantageous side of phased array technology is that direction of main beam of the antenna can be controlled by adjusting the phase between different antennas [33]. The development in array technology is continued in the concept of adaptive arrays. In adaptive antennas, both of the gain and the phase of the signals induced on the elements are changed to adjust the gain of the array in a dynamic fashion, as required by the system [2, 33]. Consequently, the array adapts to the situation required for the system [2].

Nowadays, the mobile systems are developed so that operate over two or more frequency bands and consequently, the need for antenna arrays operating in more than one frequency band are emphasized. Then, the role of array antennas which have ability to operate at the two frequencies is highlighted [34]. Nowadays, the smart antennas have achieved more attention due to their configurability's. In fact, smart antenna structure is based on the use of an adaptive antennas array, consisting of elements whose outputs are adaptively combined through a set of complex weights. Although, these operations improve the system's performance but, adaptive antennas have high implementation costs and complexity limitations [2, 35].

2.4 Application of Array Antennas in Mobile Communication Systems

Array antennas have been used in different aspects of mobile communications including base-mobile and satellite-to-mobile communication systems.

In the base-mobile system, a base station situated in a cell to communicate multiple mobile systems within the cell. Therefore, it is required to use array antenna providing adaptive beams to find the location of each mobile, and then the beams are formed to cover different mobiles or group of mobiles. The beams are also shaped to cover the cell considering the traffic in different sections of the cell as well as moderating the energy. Besides directing the beams toward the mobiles, the system may be able to adjust the pattern having nulls toward other mobiles to reduce the undesirable interferences in both receive and transmission mode[2].

The array antennas used for satellite mobile communications are divided into two categories including the antennas mounted on board of the satellite and the antenna mounted on the mobile. The array antenna mounted on the satellite is able to provide the beam-generation facility, resulting in different forms of beams depending on the requirements of the system. It can be used in generating spot beams of varying shapes and sizes dictated by positions of the mobiles. Consequently, this will reduce the transmitted power, relaxing the need to generate large amounts of power onboard of a satellite. The ability of adapting beam shapes is also useful in reducing the interference. In the mobile or terrestrial side, directive array antennas can be used to reduce interference from other neighboring satellites by pointing the beam in only required direction or desired satellite [2].

In fact, variable combinations of elements with variable weighting generate required beams in the desired direction [2]. This concept may be used in both satellite antenna or ground station, with ability to reduce interferences in such satellite systems having large number of channels. Chapter 5 of this thesis proposes the directive properties of Binomial array which can be used for this aim.

2.5 Feeding Techniques

Feeding of the array elements may be accomplished by a variety of methods. For a 4 × 4 planar array antenna, different feeding arrangements are shown in Figure 2.3[36, 37]. The main difference between the four methods in Figure 2.3 is feeding phase

difference between the elements. For instance, all the elements in Figure 2.3d are fed with equal phases, where the elements placed along any row of the array in Figure 2.3a are fed with different phases. Another difference between the feed networks is the number of power splitters used in the feed networks.

(a) (b) (c) (d)
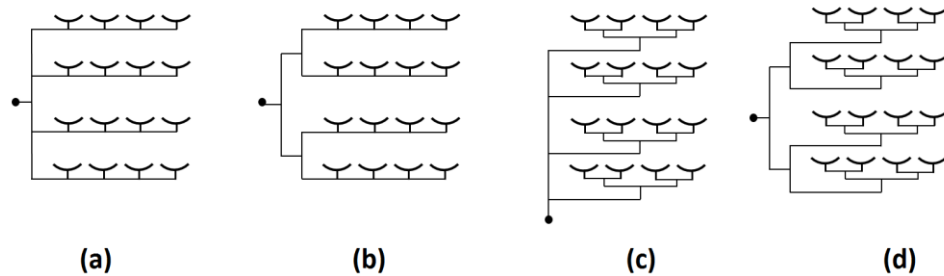
Figure 2.3 : Different feeding networks.

Microstrip antenna has been widely used in various applications due to its special features. However, it also suffers from some drawbacks, especially its low efficiency. One of the common challenges in designing a planar array antenna is the loss in the feeding network. Using high number of elements such as in Figure 2.3, causes to loss in increased transmission line lengths. In these years, a lot of efforts have been done to solve this problem. Most suitable choice would be hybrid microstrip and waveguide feed system, but the size of the corporate feed for the sub-array must be carefully determined. In [7] waveguide-fed planar antenna array is proposed and designed for Ku band direct broadcast from satellite reception for mobile systems. Prototype of a waveguide-based feed network is shown in Figure 2.4.

However, in comparison with the advantages of waveguide-fed arrays, their size and fabrication costs are considered as the man disadvantages of this approach.
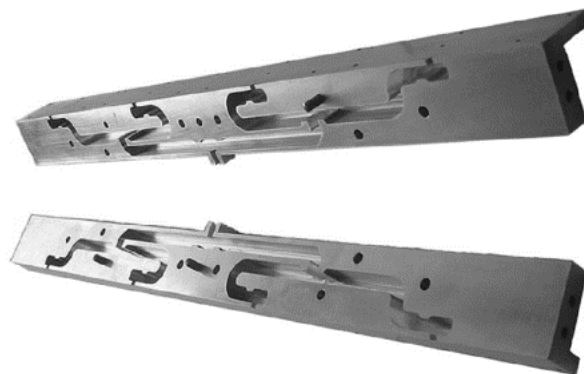
Figure 2.4 : A Waveguide feed network [38].

2.6 Different Array Structures

In one category, arrays are divided into two broadside and end-fire arrays. In broadside arrays, the maximum radiation of the array directed normal to the axis of the array. Advantage of the broad side array over the end-fire array is its steerable beam which can be used in several applications such as radars. Radiation of the end-fire array is along the axis of the array.

In another category, arrays are organized with their nonuniform excitation, such as Binomial and Dolph-Tschebyscheff arrays. Binomial array may be preferred as an advantageous approach in array antenna design having minimum SLL. In fact, binomial arrays with element spacing smaller than one-half of a wavelength [27] do not exhibit any minor lobes. Therefore, it can be considered for use in applications where SLL plays a crucial role in the system. However, there are no compact expressions for the array factor and directivity for binomial arrays of any spacing between the elements except for $\lambda/2$ spacing. However, in Chapter 5 a method is proposed for this aim.

In comparison with Binomial array, the Dolph-Tschebyscheff array is proposed as the most practical approach in array design with small side lobes. In fact, Dolph used Tschebyscheff polynomials to obtain the excitation coefficients to determine the optimal weights for linear, equally spaced arrays which is published in 1946 [39] known as the Dolph-Tschebyscheff method.

In comparison with Binomial and Dolph-Tschebyscheff arrays which are based on arrays with linear spacing but nonuniform amplitudes, others modification based on geometry considerations are proposed. The first research is introduced in 1960s proposing the improvement in array performance via geometry optimization. Based on Unz study [32], in 1960, performance of the array can be improved by holding the weights constant and varying the element positions. In 1960, King [32] proposed eliminating grating lobes via element placement in an array. In 1961, Harrington [40] considered small element perturbations to obtain a desired array pattern. A simple method of nonuniformly spaced linear array design based on Gaussian quadrature is introduced by Stutzman [41]. Array geometry optimization has been also under investigation recently using biologically inspired algorithms, such as Genetic Algorithms (GA).

3. APPLICATION OF ANTENNAS IN SATELLITE COMMUNICATIONS

Subject of this study is Ku band, where the range between 1 GHz and 60 GHz is dedicated to commercial satellite communications[3].

3.1 Directional Properties of Antennas

At a fixed radius from an isotropic source, which defines a sphere, the power density is uniformly distributed over the surface of the sphere regardless of direction. Then, density of the power radiated over the sphere of radius r is calculated by (3.1)[27].

$$W = \frac{p_{rad}}{4\pi r^2} \quad (W/m^2)$$

(3.1)

where, W is power density at distance r of the isotropic source and p_{rad} is the total radiated power.

As seen from (3.1), density of the power at a distance decreases by $1/r^2$ as the point of reception moves farther away from the source. Consequently, the challenge of antenna design is to maximize the fraction of energy that the transmitter antenna actually delivers to the receiver in long range communications. Then, concept of directive antennas are arisen to increase the effective aperture of antennas. Directivity of an antenna in a given direction is defined as the ratio of the radiation intensity in this direction to the radiation intensity averaged over all directions as in (3.2) [27].

$$D(\theta, \phi) = \frac{U(\theta, \phi)}{\frac{p_{rad}}{4\pi}}$$

(3.2)

where, $D(\theta, \phi)$ is the directivity in a given direction and $U(\theta, \phi)$ is radiation intensity in that direction that is defined as the radiated power per unit solid angle.

Also, unit solid angle (steradian) is defined as the solid angle whose vertex is at the center of a sphere with redius r that is subtended by a spherical surface area equal to

that of a square with dimension of r. Also, element of the unit solid angle of a sphere $d\Omega$ is defined as (3.3). Angles θ and ϕ are considered as in Figure 2.2 with respect to z and x axes, respectively.

$$d\Omega = \sin\theta \ d\theta \ d\phi \qquad (3.3)$$

In fact, the effective aperture of an antenna is related to its directivity by (3.4) [27]. The more the directivity increases, the more the aperture efficiency increases.

$$A_{eff} = \frac{\lambda^2}{4\pi} D \qquad (3.4)$$

where, A_{eff} is effective aperture of the antenna, λ is wavelength ans D is directivity of the antenna.

For typical dish antennas, amount of the efficiency varies between 55% and 70%.

By using directive antennas, it is possible to concentrate the energy towards the necessary directions. In other words, it is the critical parameter describing the ability of antenna in suppressing interferences from unwanted directions. An antenna radiation pattern with a main beam, side lobes and a back lobe is shown in Figure 3.1. For comparison, the uniform pattern of an isotropic source is superimposed to scale on the directional antenna pattern.
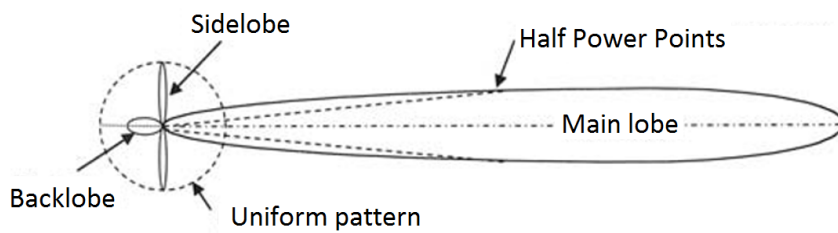
Figure 3.1 : Radiation pattern of a directive antenna [3].

3.2 Beamwidth and Sidelobes

The HPBW is the angular width of the main beam measured between the points where the power intensity is one-half that of the peak. In other words, the half power point is where the directivity is 3 dB down. Assuming that the microwave link can still function with a 3-dB decrease in signal strength, the HPBW defines the range of antenna pointing over which the antenna or satellite can move. However, only a 0.5-dB drop

14

in signal power is suggested, which demands either tighter antenna pointing accuracy or satellite position control[3].

In the previous section, the advantages of directive antennas in long range communications is provided. For planar array antennas, directivity is related to HPBW as in (3.5)[27]. However, this approximate is accurate where, the intensity of minor or side lobes are very low.

$$D \approx \frac{32400}{\theta_1 \theta_2}$$ (3.5)

where, θ_1 and θ_2 (in degrees) are HPBW of the radiation pattern in two perpendicular planes.

Most of the available designs are accomplished with aim of increasing directivity according to (3.5). Although, the proposed approaches in this thesis are also aimed to design array antennas with high number of elements to increase the directivity. However, in some applications it may be required to use very narrow beams to overcome unwanted interference, without needing to increase the directivity (by lowering SLL) based on (3.5). For instance, the novel method in section 4.3 of this thesis is developed for this aim to achieve narrow beams without increasing the directivity.

Side lobes of antennas may be additional sources of interference. Radiation pattern of a 10-element antenna in term of directivity is demonstrated in Figure 3.2.
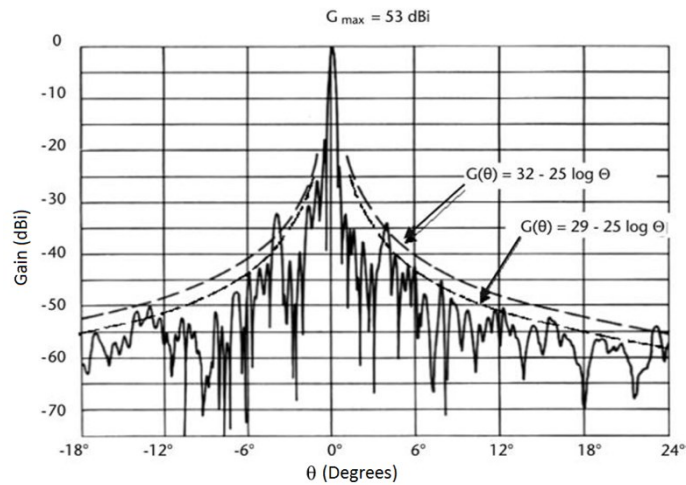
Figure 3.2 : A comparison of the radiation pattern of a real 10-element C-band antenna with the ITU sidelobe envelope [3].

In Earth station antennas, sidelobes and backlobs are important characteristics which can lead to interference in transmission or receive modes. A smooth curve called sidelobe envelope defining the specification of maximum sidelobes is demonstrated in Figure 3.2.

3.3 Isolation

The directive property of an antenna determines how effective it will be for getting signal power from the source to the receiver. However, as it was shown in the previous section, side lobes may lead to an interference effect causing to degrade a link by signals on the same frequency. Same as in reception, a transmitting station can cause degradation to other systems by sidelobe radiation. Techniques such as beam shaping, cancelation, and shielding are developed to overcome this drawback. The interference can also be optimized in acceptable limits by using isolation by natural (geographical or angular/orbital separation) or artificial (shielding or beam cancellation) approaches. This interference is more critical in satellite communications. But, by using directional ground antenna it is useful to focus on one particular satellite, suppressing the interference produced by adjacent satellites. Therefore, several satellites can operate in the geostationary arc in the same frequency band same as in Figure 3.3.
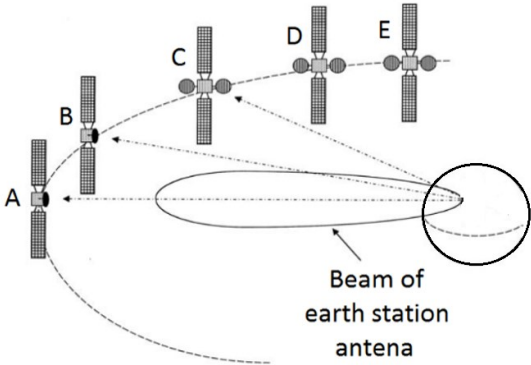
Figure 3.3 : Improved GEO arc utilization by using earth station antenna having narrow beam [3].

The specification shown in Figure 3.2 as the sidelobe envelope defines the worst case potential for interference which can be used in practice. The (3.5), which was adopted by the International Telecommunication Union (ITU) as Recommendation S.465-5, provides a common standard for the larger ground antennas used at C and Ku bands. In it, gain at a particular off-axis angle is specified in the direction of a potentially interfering (or interfered-with) satellite by (3.6) [3].

16

$$G(\theta) \leq 29 - 25 \, \log_{10} \theta \, , \quad dBi \tag{3.6}$$

where θ is the offset angle between the direction of the main beam and that toward the interfering or interfered-with satellite, for angles between ± 1 degree and ± 37 degrees.

3.4 Satellite Antennas

Although, reflector antennas provide considerable aperture efficiency. However, array antennas are mostly recommended due to their different advantages and applications, which some of them are provided in Chapter 2 of this thesis. The use of array antennas have provided more complicated performances such as beam steering, beam shaping and configurability of the beam. It may be aimed to achieve a desired beam by selecting proper weighting of the elements as an effective approach in suppressing interferences. Therefore, arrays antennas have multiple advantages over reflector and other type.

Microstrip technology is widely used in order to design satellite antennas. Although, performance of the microstrip antennas are limited and also efficiency of microstrip antennas are low, But array of microstrip antennas are widely proposed to be used in satellite technology. This is preferred mostly in the design of receive station structure. The most desirable characteristics which leads to wide use of microstrip antennas are their low weight and low fabrication costs. As a typical model, a TX/RX 4x4 elements passive Sub-Array of a larger array antenna designed for Ku band is demonstrated in Figure 3.4a [42].

(a)   (b)
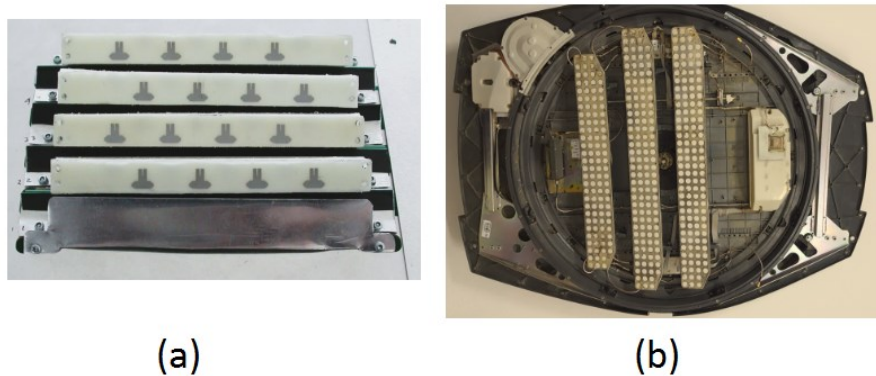
Figure 3.4 : Array structures based on microstrip technology (a) a sub-array of a larger array antenna designed for Ku band [39] (b) Raysat array antenna for KU band in RF Lab. of Istanbul Technical University.

The antenna is low-profile and is designed for integration in small aircrafts and ground vehicles. The beam steering is electronic for the elevation and polarization angles and mechanical for the azimuth scan. In Figure 3.4b, another larger array with about 512 elements is demonstrated which includes four sub-array with mechanical steering in both planes.

Besides, arrays with waveguide feed network have attracted high attention due to their high efficiency. The wave guide network can be used as both feed network or as the antenna with apertures operating in the frequency of interest. A typical example of a waveguide array antenna with slot apertures designed for Ku band is demonstrated in Figure 3.5[43].

Figure 3.5 : Prototype of a waveguide-fed array antenna for KU band[43].

4. THREE NOVEL METHODS OF ARRAY ANTENNA DESIGN

Based on the application of interest, it is required to improve dimensions, efficiency or HPBW of the antenna. Although, there are several designs available for these aims. But, most advantages of the methods proposed in this Chapter are their simplicity and low cost in terms of practical use and fabrication. In fact, the improvements are achieved by using effective array factors and special elements. Section 4.1 proposes a novel design with desired directive property but having smaller aperture compared to available designs. Section 4.2 introduces a novel method to design an array with reduced number of elements. Finally, a new method to achieve a narrow beam width is offered in section 4.3.

4.1 Novel Array Antenna Design with Small Aperture

All the designs in [38] and [44-47] have used conventional method of array design with λ element spacing (or the range between 0.7λ and λ) independent of properties of the element antennas to achieve a beam with narrow main lobe and to avoid the second and third strong lobes. This region of element spacing is also recommended by ITU in [48]. Unlike those arrays, procedure in this section is developed on optimizing the array factor based on the properties of a special element.

In Figure 2.1 in Chapter 2, an array with two elements on the z axis is demonstrated. Normalized array factors for this array with λ and $\lambda/2$ spacing's are demonstrated in Figure 4.1a and Figure 4.1b, respectively. Designs in [38] and [44-47] use λ element spacing to achieve a minimum beam width for the lobe at $\theta = 90°$, although having side lobes at $\theta = 0°$ and $\theta = 180°$ as in Figure 4.1a. In fact, the main lobe of the array factor at $\theta = 90°$ would be narrower by enlarging the element spacing from $\lambda/2$ to λ. The element antenna with conventional beam as in Figure 4.1a has been used with nulls at $\theta = 0°$ and $\theta = 180°$ to cancel the side lobes of the array factor.

Considering Figure 4.1a and Figure 4.1b, main lobe of the array factor at $\theta = 90°$ with smaller spacing is wider than the lobe of array factor with larger spacing. But, the array

factor in Figure 4.1b has the advantage of having a single lobe without unwanted side lobes by its own shape. Therefore, element antennas with a very directive lobe at $\theta = 90°$ along with side lobes at any other directions can be used to achieve the same directivity obtained by the conventional approach, but with a smaller size. More clearly, it seems that forms of the element factor and array factor in conventional designs (in Figure 4.1a) are changed in this approach (in Figure 4.1a). Directivity of the conventional element antennas with single lobe such as in Figure 4.1a can be increased up to a limited value. But, it may be possible to design element antennas with a very narrow lobe at $\theta = 90°$ along with having any unwanted lobes at other directions (which will be canceled using $\lambda/2$ spacing arrays), demonstrated as the element factor in Figure 4.1b. In fact, the array factor is chosen corresponding to the properties of the special element antenna.
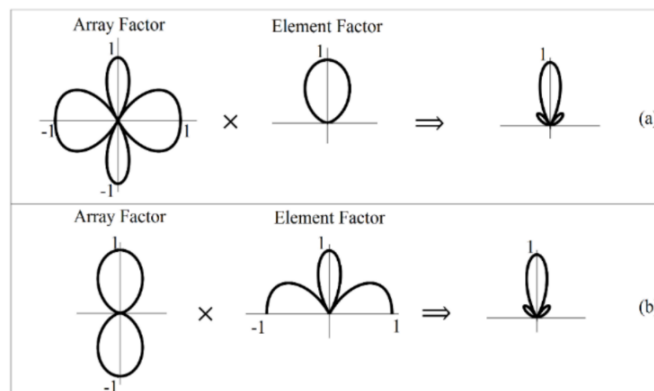
Figure 4.1 : (a) Two-element array with λ spacing (b) two-element array with 0.5λ spacing and using a special element.

In Figure 4.2, radiation patterns of the antenna proposed in [49, 50] with and without a parasitic element in H-Plane are demonstrated.
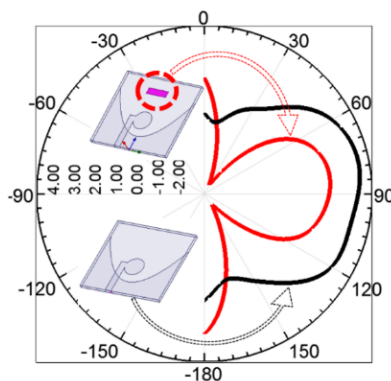
Figure 4.2 : Radiation pattern of the element antenna proposed in [49, 50] with and without the parasitic element at the frequency of 11 GHz.

Beam of the antenna without the parasitic element includes a single lobe with maximum at $\theta = 90°$ such as the element factor in Figure 4.1a. However, beam of the same antenna with the parasitic element demonstrated by red highlight in Figure 4.2 is changed so that two nulls are appeared at $\theta = 30°$ and $\theta = 150°$. Also, the main lobe at $\theta = 90°$ is narrowed and the side lobes at $\theta = 0°$ and $\theta = 180°$ are enlarged such as the element factor demonstrated in Figure 4.1b. Then, those unwanted side lobes can be canceled by using the array factor demonstrated in Figure 4.1b with $\lambda/2$ spacing.

The antenna demonstrated in Figure 4.2 is a modified form of the antenna in [49, 50] which is designed with smaller dimensions for Ku band. Gain of the antenna without the parasitic element is 4.5dBi and with the parasitic element at $\theta = 90°$ is 3dBi. Array designs with $\lambda/2$ and λ spacing with and without the parasitic element, respectively based on this element are compared to each other in Figure 4.3. In the conventional method (λ spacing), the gain is increased up to 2.5dBi from 4.5dBi to 7dBi. But, gain of the antenna is increased up to 4.5dBi from 3dBi to 7.5dBi by using the novel approach.
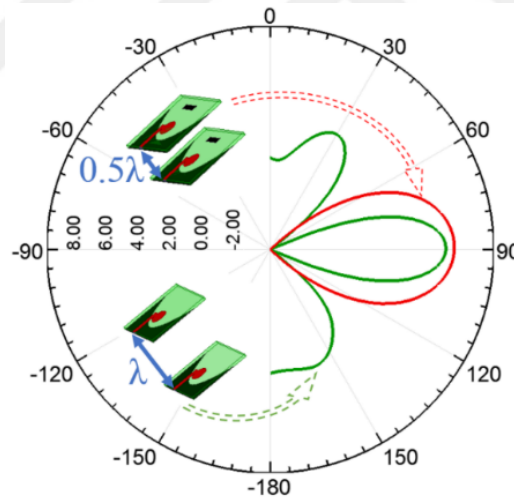
Figure 4.3 : Radiation pattern of the two-element array (array of element antenna proposed in [49, 50]) with and without a parasitic element with different spacing's at the frequency of 11 GHz.

HPBW of the array with λ spacing is smaller than the array with $\lambda/2$ spacing due to fact that the antenna with the parasitic element has no ideal expected radiation properties with a very narrow lobe at $\theta = 90°$. However, the larger slope of gain raise (4.5dBi) by using the novel method in comparison with the conventional approach (2.5dBi) confirms the accuracy of the approach. Spacing in the array in Figure 4.1b is half of the spacing in Figure 4.1a.

This approach can be also accomplished in the next step for four-element arrays. The same improvement could be accomplished only if the array of two elements includes two unwanted side lobes which can be eliminated by using the proposed method. Subsequently, the two-element arrays with $\lambda/2$ spacing demonstrated in Figure 4.3 may be considered as new element antenna to design another two-element array (four-real-antenna but two new-elements) with 2λ spacing from center of the new element antennas (demonstrated in Figure 4.4c) . But, both array factors with 2λ and λ spacing's produce large lobes at $\theta = 0°$ (as is demonstrated in the following in Figure 4.8 for 8-element array that is the same for 2-element array). Consequently, the spacing can be reduced from 2λ to the range between λ and 2λ depending on the properties of the new element antenna.

Simulation of the four-element array with different spacing's are demonstrated in Figure 4.4.
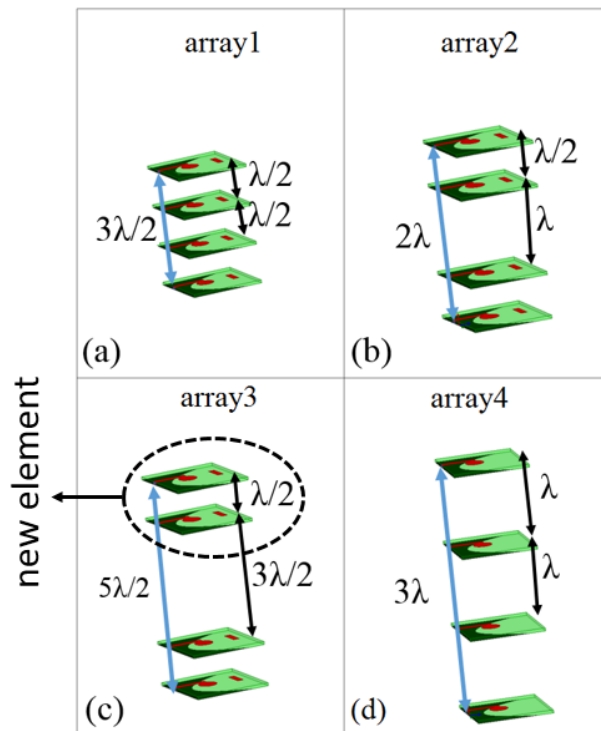
Figure 4.4 : (a), (b) and (c) four-element arrays with λ, $3\lambda/2$ and 2λ, spacing's respectively, between centers of the two new element antennas, (d) conventional four-element array with λ spacing.

Figure 4.4d demonstrates a conventional array of 4 element antenna with λ element spacing. In Figure 4.4a, Figure 4.4b and Figure 4.4c, several arrays are demonstrated with different spacing's between the elements. In these Figures, the proposed two-

element array (based on the novel approach) in Figure 4.3 is considered as the new element antenna.

Radiation pattern of those arrays demonstrated in Figure 4.4 are demonstrated in Figure 4.5 in H-plane at the frequency of 11 GHz. HPBW and dimension of all the arrays are demonstrated in Table 4.1.
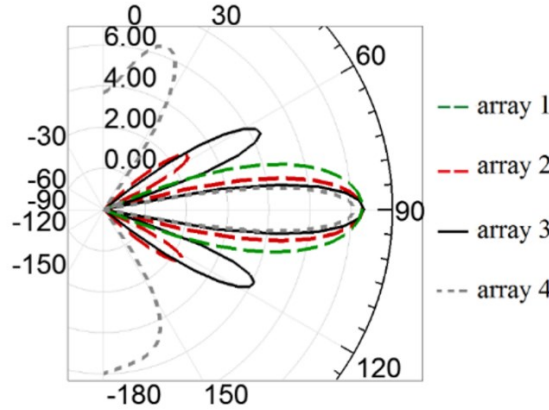
Figure 4.5 : Radiation pattern of the antennas demonstrated in Figure 4.4, in H-plane, at the frequency of 11 GHz, simulated in HFSS.

Table 4.1 : Characteristics of the beams demonstrated in Figure 4.5.

Array structures	Size (λ)	HPBW(degrees)	Gain (dBi)
Array1	1.5 λ	26°	10.5
Array2	2.0 λ	18°	10.5
Array3	2.5 λ	14°	10.6
Array4	3.0 λ	13°	10.2

For arrays 2 and 3 demonstrated in Table 4.1, HPBW values are desiable compared to that 13° value achieved by array4, considering that the aperture sizes are smaller than that of array4. However, the beam width can be more improved by the use of a more ideal special element antenna. It is tried to use two similar antenna structures to maintain the accuracy of this study. But, the more the ideal special element is used, the more the ideal results can be achieved.

4.2 Novel Array Antenna Design with Reduced Number of Elements

Array antennas with high number of elements are developed to obtain high directivity, and low side-lobes. Microstrip technology has been widely investigated for use in array antenna designs having the drawback of dielectric and ohmic losses in the feeding network [6,7]. On the other hand, the use of large number of power splitters

leads to increase of insertion or isolation loss in the power-splitting [8,9]. Therefore, optimization of feed network of large arrays have been investigated extensively to shortening the strip lines or lowering the number of power splitters. Serially fed network system is proposed to reduce the number of power splitters which is not an ideal method. Waveguide feeding [12,13] also is not a cost effective method. In this section a new approach is proposed to reduce the number of elements and consequently, reduce the number of power splitters.

In all available designs such as in [38] and [44-47] an element spacing equal or less than λ is used to discard the drawback of minor lobes. However, the arrays based on directive elements such as in [51] can be designed by using reduced number of elements with larger spacing than λ, resulting in the same HPBW achieved with λ spacing. Then, number of power spliters will be reduced.

Consider a linear array of N elements with d spacing along the z-axis as in Figure 4.6 (In this figure odd number of elements are shown and the reference point in Figure 4.6 is taken at the physical center of the array).
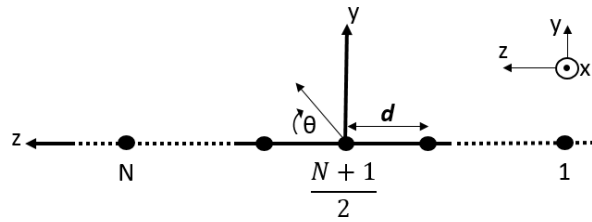
Figure 4.6 : Uniform linear array of N elements.

Then, normalized array factor of equally spaced N elements (odd or even) with uniform and unity excitation can be written as (4.1) [27].

$$AF_N(\theta) = \frac{1}{N} \sum_{n=0}^{(N-1)} e^{j\left[n-\left(\frac{N-1}{2}\right)\right]\psi}$$

(4.1)

where:

$$\psi = k \,.\, d \,.\, cos\,\theta + \beta$$

(4.1a)

$k\left(\frac{2\pi}{\lambda}\right)$ is the wave number and d and β (is considered as zero in this thesis) are the spacing between the elements and the progressive phase shift, respectively.

24

Where, the aperture distribution on Z axis for discrete elements can be written as (4.2).

$$I_N(z) = \sum_{n=0}^{(N-1)} \delta\left(z - \left[n - \left(\frac{N-1}{2}\right)\right] d\right) \tag{4.2}$$

where:

$$\delta(z) = \begin{cases} 1 & z = 0 \\ 0 & z \neq 0 \end{cases} \tag{4.2a}$$

The value of $\delta(z)$ at $z = 0$ is considered as 1 as a representative value of its area (normalized value)[52]. In (4.1), the array factor includes expressions for any of the elements. Where, transforming (4.1) to a multiplication form reduces the number of those expressions as well as simplifying the analysis of the array factor. For this aim, Fourier transform can be used as the effective method. Since the array factor is related to the aperture distribution through an inverse Fourier transform [27,53,54], the aperture distribution of a favorably determined array factor can be derived through a direct Fourier transform. It can be simply seen that array factor in (4.1) is formally the inverse Fourier transform of the aperture distribution in (4.2). Then, by using the multiplication property of the Fourier transform [52], if an aperture distribution is indicated by convolution of minor expressions then, the array factor can be expressed by multiplication of minor array factors corresponding to those minor expressions. Consider a linear array of 8 elements. Then, the aperture distribution I on Z axis can be demonstrated same as in Figure 4.7.
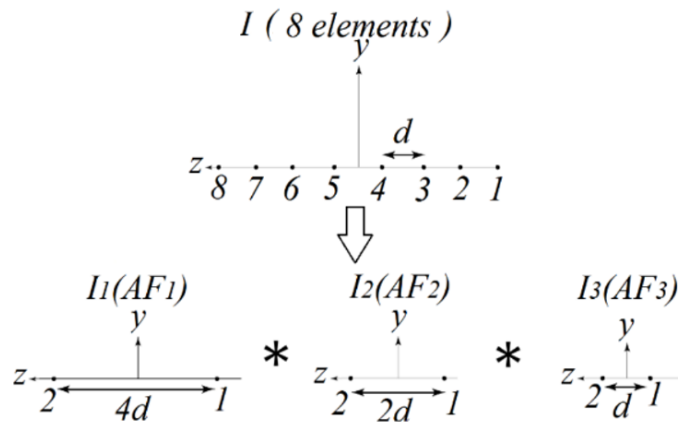
Figure 4.7 : Distribution of 8-element linear array in the form of two convolutions of minor components I_1, I_2 and I_3.

Considering the shifting property of convolution of a hypothetical function $f(z)$ with $\delta(z)$ as in (4.3) [52],

$$f(z) * \delta(z - z_0) = f(z - z_0) \tag{4.3}$$

and taking into account that:

$$\delta(z \pm z_0) = \delta(z + z_0) + \delta(z - z_0) \tag{4.3a}$$

accuracy of the convolutions in Figure 4.7 is demonstrated in (4.4).

$$I_1 * I_2 * I_3 = \delta(z \pm 2d) * \left[\delta(z \pm d) * \delta\left(z \pm \frac{d}{2}\right) \right] = \tag{4.4}$$

$$\delta\left(z \pm \frac{d}{2}\right) + \delta\left(z \pm \frac{3d}{2}\right) + \delta\left(z \pm \frac{5d}{2}\right) + \delta\left(z \pm \frac{7d}{2}\right) = I_{8-\text{elements}}$$

where,

$$\begin{cases} I_1 = \delta(z \pm 2d) \\ I_2 = \delta(z \pm d) \\ I_3 = \delta\left(z \pm \frac{d}{2}\right) \end{cases} \tag{4.4a}$$

Then, the normalized array factor for the array shown in Figure 4.7 can be written as (4.5).

Also, each of the minor array factors AF_1, AF_2 and AF_3 are based on (4.1).

$$AF = (AF_1) . (AF_2) . (AF_3) = \tag{4.5}$$

$$\left[\cos\left(4\pi \frac{d}{\lambda} \cos\theta \right) \right] . \left[\cos\left(2\pi \frac{d}{\lambda} \cos\theta \right) \right] . \left[\cos\left(\pi \frac{d}{\lambda} \cos\theta \right) \right]$$

Array factor in (4.5) with different element spacing's d is demonstrated in Figure 4.8. The more the element spacing increases in Figure 4.8 the more the main lobe at $\theta = 90$ would be narrower. HPBW values for arrays with same aperture length but different number of element and spacing between the elements confirms that aperture length of the array is the major parameter determining HPBW. This concept is used to reduce the number of interior elements in an array. But, it is seen in Figure 4.8 that the

additional lobes appear besides the main lobe at $\theta = 90°$ by using the element spacing larger than λ. In other words, additional lobes are made by elimination of intertwined elements. This undesirable side lobe can be eliminated by the use of a directional element.
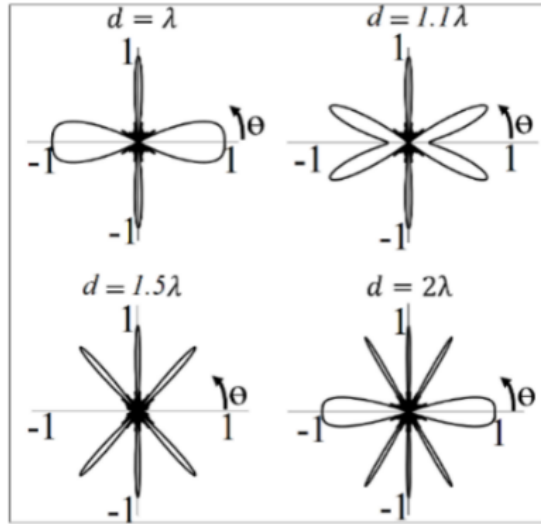
Figure 4.8 : Array factor of the two-element array with different spacing's d.

To better demonstrate the approach, a comparison between two arrays with 8 and 16 elements with 2λ and λ spacing's, respectively is presented. Aperture distribution of a 16-element array with λ element spacing is indicated in Figure 4.9, similar to the array in Figure 4.7.
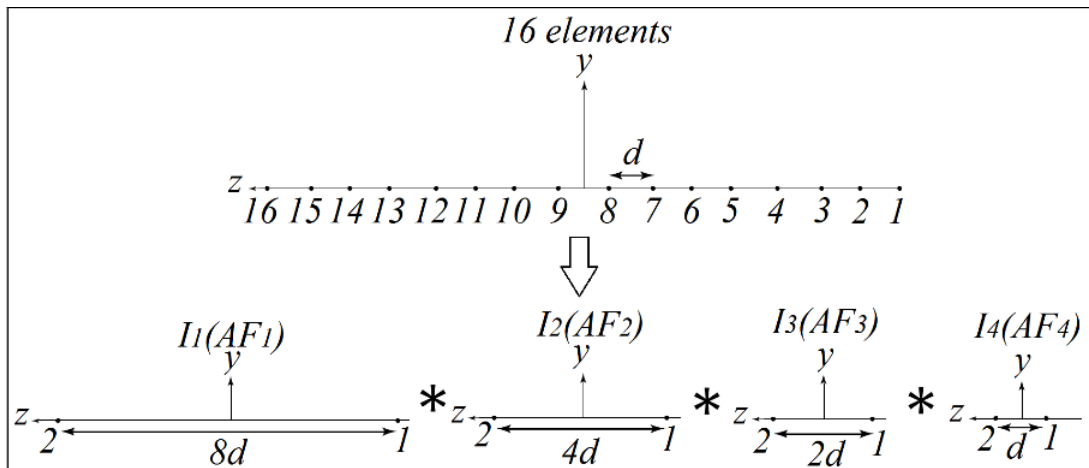
Figure 4.9 : Distribution of 16-element linear array in the form of three convolutions of minor components I_1, I_2, I_3 and I_4.

Therefore, the array factor for the array in Figure 4.9 is presented by (4.6).

$$AF = (AF_1) . (AF_2) . (AF_3). (AF_4) =$$ (4.6)

$$\left[\cos\left(8\pi\frac{d}{\lambda}\cos\theta\right)\right] . \left[\cos\left(4\pi\frac{d}{\lambda}\cos\theta\right)\right] .$$

$$\left[\cos\left(2\pi\frac{d}{\lambda}\cos\theta\right)\right] . \left[\cos\left(\pi\frac{d}{\lambda}\cos\theta\right)\right]$$

Subsequently, array factor for 8 elements with 2λ spacing can be demonstrated by the same (4.6) without the component(AF_4). The array factors corresponding to each of the elements $(AF_1), (AF_2), (AF_3)$ and (AF_4) are demonstrated in Figure 4.10. Multiplication of those components with and without (AF_4) corresponds to the array factor of 16 (with λ spacing) and 8 (with 2λ spacing) elements, respectively.
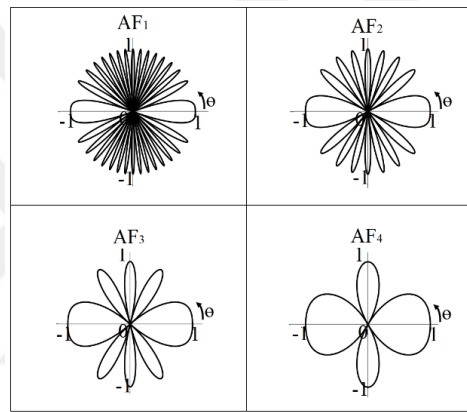
Figure 4.10 : Array factors corresponding to I_1, I_2, I_3 and I_4 indicated in Figure 4.9.

Respective multiplication of those elements are demonstrated in Figure 4.11 to better show the role of intertwined elements on the array factor.
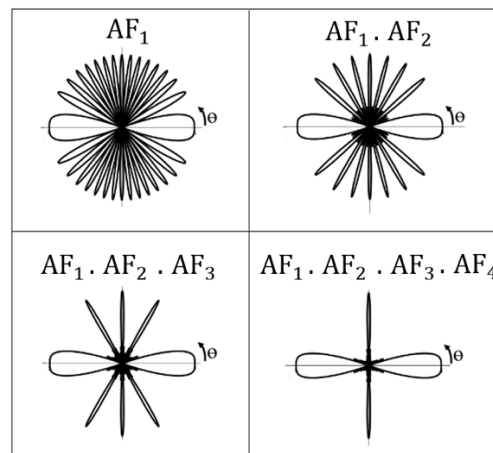
Figure 4.11 : Respective multiplication of minor elements of distribution of 16 elements demonstrated in Figure 4.9.

Then, it can be simply seen from Figure 4.11 (the change from (AF_1) to $(AF_1).(AF_2).(AF_3).(AF_4))$ that respective intertwining additional elements between the two largely spaced elements leads to elimination of undesirable lobes. Multiplying $AF_2 . AF_3$ to AF_1 leads to elimination of all undesirable beams except from that in $\theta = 60°$ (Figure 4.11), while final multiplying with AF_4 eliminates all the minor beams (Figure 4.11). Therefore, major role of the intertwined elements are in elimination of undesirable lobes. HPBW for main lobes of those minor array factors shown in Figure 4.10 are provided in Table 4.2. Those values confirm a regular widening in main lobe of array factors from AF_1 to AF_4. The great value of 28.96° for HPBW of AF_4 compared to 3.58° for HPBW of AF_1 confirms that the beam of AF_4 is wide enough to neglect improvement in HPBW of AF_1 multiplying to AF_4. This can be better shown by providing a comparison between normalized intensities of those minor array factors. Intensity of those array factors at $\theta = 88.21°$ (θ_{3dB} for AF_1) is demonstrated and compared to each other in Table 4.3. Those values of Table 4.3 are demonstrated in Figure 4.12a. It reaches to constant value of 1 through AF_3 to AF_4 after sharp rise from AF_1 to AF_3. Thus, multiplication of AF_4 with normalized intensity of $0.9951 \cong 1$ at $\theta = 88.21°$ (θ_{3dB} for AF_1) does not improves the HPBW of AF_1.

Table 4.2 : HPBW of main lobe of minor array factors demonstrated in Figure 4.10.

Array factors	HPBW(degrees)
AF_1	3.58
AF_2	7.14
AF_3	14.38
AF_4	28.96

Table 4.3 : Normalized intensity of minor array factors demonstrated in Figure 4.10 at $\theta = 88.21$ (θ_{3dB} for AF1) degrees.

Array factors	Normalized intensity
AF_1	0.707
AF_2	0.9231
AF_3	0.9806
AF_4	0.9951

Consequently, convolution of array distributed by $I_1 * I_2 * I_3$ (8 element with 2λ spacing) with I4; in other words, intertwining more elements between elements of array distributed by $I_1 * I_2 * I_3$ does not improve the HPBW. This is finally confirmed by values provided in Table 4.4 where HPBW values after respective multiplication of

minor array factors are demonstrated. In Figure 4.12b and Table 4.4 the amount of HPBW value sharply drops from $3.582°$ in AF_1 to $3.154°$ in $(AF_1).(AF_2).(AF_3)$. Then, it tends to reach approximately constant value through $3.154°$ to $3.142°$. In other words, those amounts of $3.142°$ and $3.154°$ HPBWs corresponding to the arrays with and without AF_4, respectively in Table 4.4 confirms that the HPBW of 16 elements with λ distance is not by far different from that of 8 elements with 2λ spacing. It should be noted that the improvement (fast drop in Figure 4.12b) in values of HPBW by convolving I_2 with I_1 or multiplying (AF_2) to (AF_1) is majorly due to enlargement in the size of array. Although, those intertwined elements can be effective in improvement of gain beam by elimination of side lobes. But, the use of a highly directive element eliminating undesirable side lobes will eradicate the need for those elements.

Table 4.4 : HPBW of main lobe of array factors demonstrated in Figure 4.11.

Array factors	HPBW(degrees)
(AF_1)	3.582
$AF_{12} = (AF_1).(AF_2)$	3.224
$AF_{123} = (AF_1).(AF_2).(AF_3)$	3.154
$AF_{1234} = (AF_1).(AF_2).(AF_3).(AF_4)$	3.142

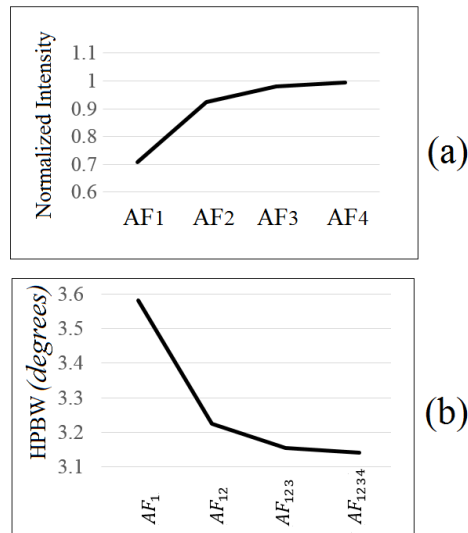**Figure 4.12 :** (a) Normalized Intensity of AF's at $\theta = 88.21$ (θ_{3dB} for AF1), (b) variety of HPBW by intertwining additional elements.

It is demonstrated that AF_1 and AF_2 are the major elements determining HPBW of the main lobe. While, major role of AF_3 and AF_4 are in elimination of minor lobes. As a result, the role of AF_4 in elimination of minor lobes can be substituted by using a

directive element. The directive element must have radiation characteristics similar to AF_4 to achieve the similar results with only main lobe at $\theta = 90°$. Direction of the minor lobe (without AF_4) is at $\theta = 60°$ and changes from $\theta = 0°$ to $\theta = 60°$ with increasing the element spacing from λ to 2λ. Therefore, the beam of the element is required to have a null at the same direction $\theta = 60°$. Several highly directional antennas such as in [50] can be used for this aim. Therefore, the array can be designed with 2λ or greater spacing to reduce the number of elements. The optimum element spacing is corresponding to the direction at which the minor lobe reaches to the null in the beam of the element. A prototype array antenna is fabricated and measured based on the results of this section that is provided in Section 4.4.

4.3 Novel Nonlinear Array Antenna Design with Narrow Beam Width

One major requirement in satellite communications is narrow beam width of the antenna to overcome interferences from neighbor satellites . In some cases, beam width of the antenna is the major determining factor (in terms of interference) and is more critical than the SLL. Therefore, a small amount of optimization in the beam width of the antenna may be effective, although resulting in reduced directivity.

In section 4.2, it is demonstrated that HPBW of the array factor is determined majorly by larger distributions I_1 and I_2 as a measure of the aperture length of the array; more clearly by the elements placed at ends of the array. Subsequent results confirmed that those additional interior elements are mostly effective in elimination or reduction of undesirable side lobes. The idea behind design of the novel nonlinear array is arisen from these observed characteristics.

In Figure 4.12, placement of additional elements corresponding to I3 and specially I_4 do not by far improves the HPBW. As the HPBW is majorly determined by I_1 (corresponding to AF_1), then nonlinear method includes enlarging the distance in minor component I_1. Convolving those other components with larger I_1 results in an optimum aperture distribution in which those inefficient interior elements are swept towards ends of the array. In order to better comparison with linear array consider the linear array demonstrated in Figure 4.13a in which 8 elements are placed with element spacing d. A nonlinear array with the same size is demonstrated in Figure 4.13b. This Nonlinear array can be displayed with two convolutions of minor elements demonstrated in Figure 4.13c. In Figure 4.13b, d_1 corresponding to I_1 is selected larger

31

than d (in linear array) to increase the density of elements towards the ends of the array. But, d_2 and d_3 corresponding to I_2 and I_3, respectively must be optimized in a way that size of both linear and nonlinear arrays become equal. Although, enlarging the spacing for I_1 cause to reduce the spacing in I_2, but improvement in HPBW due to increased I_1 is greater than increase in HPBW due to reduced I_2.

To simplify the calculation, d_3 is determined equal to d_2. Therefore, for minor elements I_2 and I_3 element spacing are $2d_2$ and d_2, respectively. The aperture distribution of the array can be demonstrated in the convolution form in Figure 4.13c same as in section 4.2.
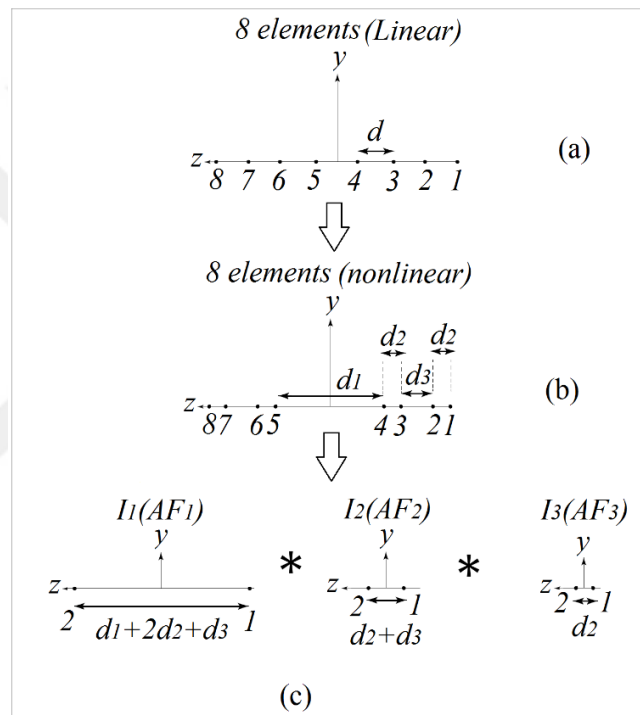
Figure 4.13 : Aperture distribution of 8 element linear and nonlinear array.

Size of the both linear and nonlinear arrays are the same as in (4.7).

$$d_1 + 6d_2 = 7d = 7\lambda \tag{4.7}$$

Same as in section 4.2, for nonlinear array in Figure 4.13b, the array factor can be written as (4.8).

$$AF = (AF_1).(AF_2).(AF_3) = \tag{4.8}$$

$$\left[\cos\left(\pi\frac{d_1 + 3d_2}{\lambda}\cos\theta\right)\right].\left[\cos\left(2\pi\frac{d_2}{\lambda}\cos\theta\right)\right].\left[\cos\left(\pi\frac{d_2}{\lambda}\cos\theta\right)\right]$$

Substituting $d_1 + 3d_2 = 7\lambda - 3d_2$ from (4.7) and $\acute{d}_2 = \frac{d_2}{\lambda}$, (4.8) can be simplified as (4.9).

$$AF = (AF_1).(AF_2).(AF_3) = \tag{4.9}$$

$$\big[\cos(\pi(7 - 3\acute{d}_2)\cos\theta)\big].\big[\cos(2\pi\acute{d}_2\cos\theta)\big].\big[\cos(\pi\acute{d}_2\cos\theta)\big]$$

Equation (4.9) is simplified to a function of parameters $\acute{d}_2$ and which distributes the properties of array factor as a function of $\acute{d}_2$ and θ. Two methods can be used to determine an optimum value for $\acute{d}_2$ resulting in narrower beam or minimum HPBW. In the first approach, substituting the normalized intensity of array factor corresponding to HPBW in (4.9) as AF = 0.707 then, (4.9) could be transformed to achieve θ_{3dB} (first θ corresponding to HPBW) as a function of a single parameter $\acute{d}_2$ as demonstrated in (4.10).

$$\theta_{3dB}(\acute{d}_2) = f(\acute{d}_2) \tag{4.10}$$

Then, applying (4.11),

$$\frac{d\theta_{3dB}}{d(\acute{d}_2)} = 0 \tag{4.11}$$

Optimum value for $\acute{d}_2$ corresponding to minimum HPBW will be obtained. However, this approach is not favorable. Then, numerical results of (4.9) can be used to follow the study. Figure 4.14 shows the HPBW of main beam versus different values of $\acute{d}_2$. It confirm the uniform drop of HPBW by regular decrease in $\acute{d}_2$. It means that HPBW of the antenna would be reduced constantly by decrease in $\acute{d}_2$. However, in the practical use it must be determined in a limited range. Therefore dimensions of individual element and coupling between adjacent elements also must be taken into account in the determination of $\acute{d}_2$.

Major drawback of the method is great side lobes in smaller amounts of $\acute{d}_2$. Same as in section 4.2, those side lobes can be controlled by the use of a directive antenna. But it is required to moderate level of those side lobes. Array factor of nonlinear array for $d_2 \acute{=} 0.7$ is compared to linear array in Figure 4.15.
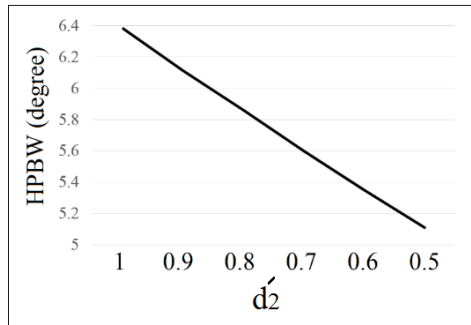
Figure 4.14 : HPBW of array versus $\acute{d}_2$ ($\acute{d}_2$ axis is inversely positioned to demonstrate the HPBW values with increase of d1 whose value inversely increase by reducing $\acute{d}_2$).
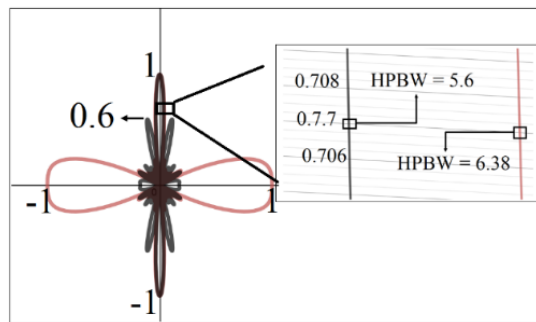
Figure 4.15 : Array factor for linear (red) and nonlinear array with $\acute{d}_2$=0.7 (black).

HPBW in Figure 4.15 is improved from 6.38° degrees to 5.6°. But, that 0.6 normalized intensity shown in Figure 4.15 for side lobes of array factor is not desirable. Normalized intensity of array factor distributed by (4.9) from $\theta = 0°$ to $\theta = 180°$ by increase of $\acute{d}_2$ from 0 to 1 is demonstrated in detail in Figure 4.16.

Figure 4.16 : Normalized intensity of nonlinear array factor in different values of $\acute{d}_2$ ($\acute{d}_2$ axis is inversely positioned to demonstrate the intensities with increase of $d1$ whose value inversely increase by reducing $\acute{d}_2$).
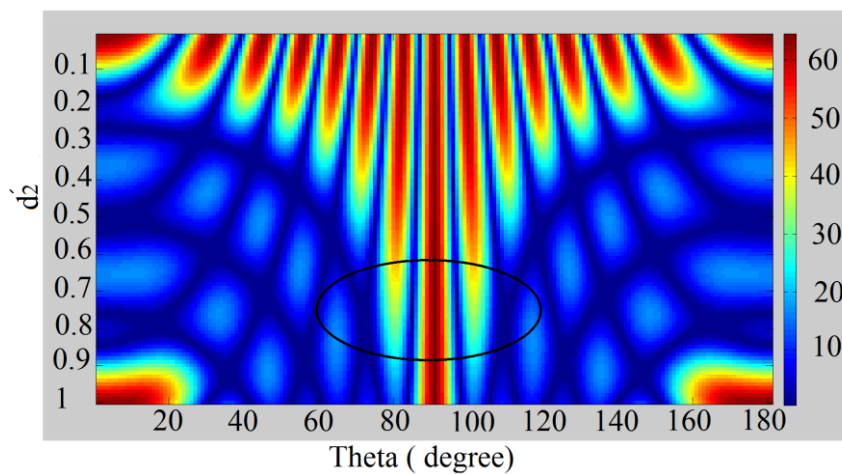
The beam width at $\theta = 90°$ narrows by decrease of $\acute{d}_2$ from 1 to 0. For $\acute{d}_2 \ll 0.4$ several side lobes are appeared throughout θ from 0° to 180°. In $\acute{d}_2 = 1$ there are only two side lobes at $\theta = 0°$ and $\theta = 180°$ corresponding to the linear array. The region encircled by black highlight $(0.7 \ll \acute{d}_2 \ll 0.95)$ describes an optimum value for $\acute{d}_2$ for nonlinear array with controlled side lobes. Although, HPBW of array factor is regularly decreased by the reduce of $\acute{d}_2$. But, optimum or minimum value for $\acute{d}_2$ is the amount at which the HPBW of gain pattern is starting to be increased due to great side lobes. It depends also on directive properties of individual element. In practical applications such as satellite communication, improvement in HPBW of gain or radiation pattern will be significant using $\acute{d}_2$ in the range $0.9 \ll \acute{d}_2 \ll 0.99$ with negligible increase in side lobe levels.

In Figures 4.15 and 4.16, two greater side lobes would be closer to the main lobe by decrease of $\acute{d}_2$. It is mentioned that an optimum value for $\acute{d}_2$ can be determined considering individual element and application of interest with minimum increase in side lobes. But, as an alternative method to overcome to this problem, (4.9) can be rewritten as (4.12) with two additional parameters k_1 and k_2.

$$AF = (AF_1).(AF_2).(AF_3) =$$

$$[\cos(\pi(7 - 3\acute{d}_2)\cos\theta)].[\cos(k_1\pi\acute{d}_2\cos\theta)].[\cos(k_2\pi\acute{d}_2\cos\theta)]$$

(4.12)

The idea behind (4.12) is arisen from the concept of previous section (changing the position of interior elements to effect the minor lobes). In other words, parameters k_1 and k_2 determines the optimum spacing for I2 and I3 corresponding to AF2 and AF3, respectively to deform the unwanted side lobes. Optimum values for k_1 and k_2 are determined as 3 and 1.5, respectively and the corresponding spacing's between the elements of array are demonstrated in Figure 4.17.

Final dimensions of this array is 8.05λ which is greater than linear array. In fact, the design uses the benefits of both concepts investigated in this section and section 4.2; more clearly nonlinear array with larger element spacing than λ.

Figure 4.18 compares two nonlinear designs based on (4.9) and (4.12). Normalized intensity of Side lobes close to the main lobe are considerably reduced from 0.6 to 0.33. In logarithmic range of gain beam that value of 0.33 is corresponding to

approximately -10 dB. Also, it is shown that the larger side lobe is swept from $\theta = 79.53°$ to $\theta = 32.44°$ which be eliminated using a directional element.
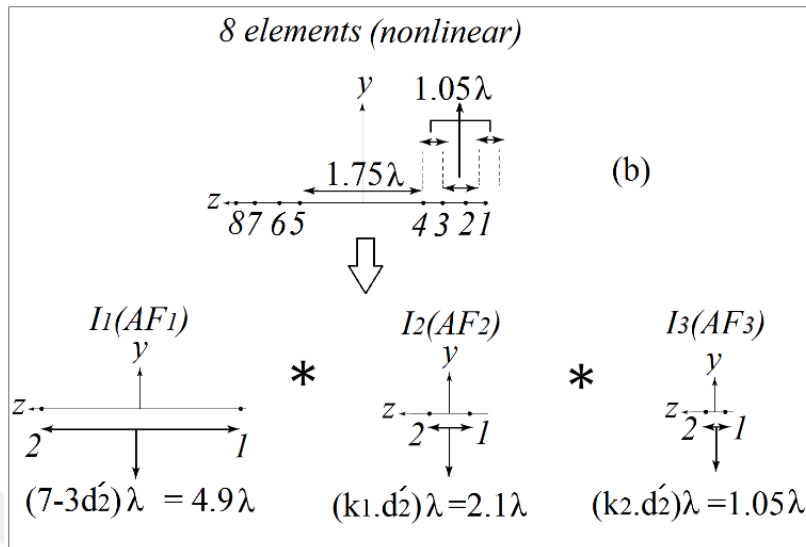
Figure 4.17 : Nonlinear array based on (4.12).
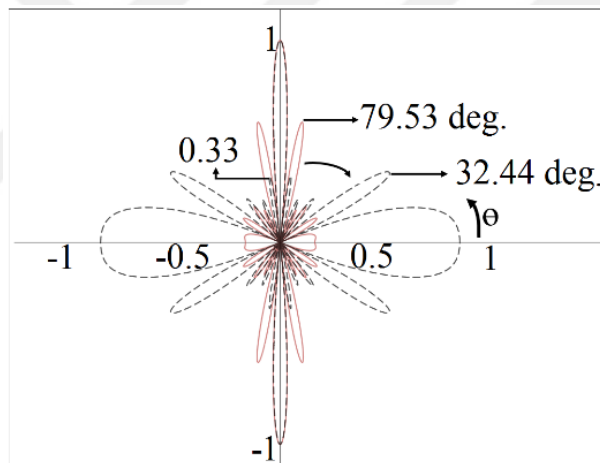
Figure 4.18 : Comparison between two nonlinear arrays based on (4.9) and (4.12).

4.4 Simulation and Measurement Results Based on Sections 4.2 and 4.3

Based on the results of section 4.2, a 8-element array antenna is analyzed and simulated by using Ansoft HFSS v.15 to confirm the results. Also, an element antenna is designed, simulated and fabricated. The 8-element array, is also fabricated based on the designed element antenna. Then, the corresponding measured results for the S11 parameters and the radiation pattern of the array antenna are provided in this section. Also, result of the method in section 4.3 is demonstrated by simulation of a planar array of the same element antenna.

36

4.4.1 Simulation of the element antenna

The element antenna used in this thesis and shown in Figure 4.19 is designed based on [50] with ideal directional properties. Consequently, dimensions of the antenna are optimized based on the results and discussion presented in [50]. Therefore, details about the optimized parameters c_1, c_2 and c_3 shown in Figure 4.19 and the other parameters in [50] are out of scope of this study and are not studied in this thesis. Those parameters are optimized to the frequency range of KU band (10-12GHz) based on the explanations in [50]. However, the unique modification in the structure of the antenna compared to [50] is its symmetry along the side of the ground plane, and subsequently, its feed approach. Then, surface current, electric fields and subsequently radiation characteristics made by the feed and circular patch are demonstrated in this section. The antenna is designed on a Taconic substrate with relative permittivity of 4.4, tan. loss of 0.003 and height of 1.02mm.
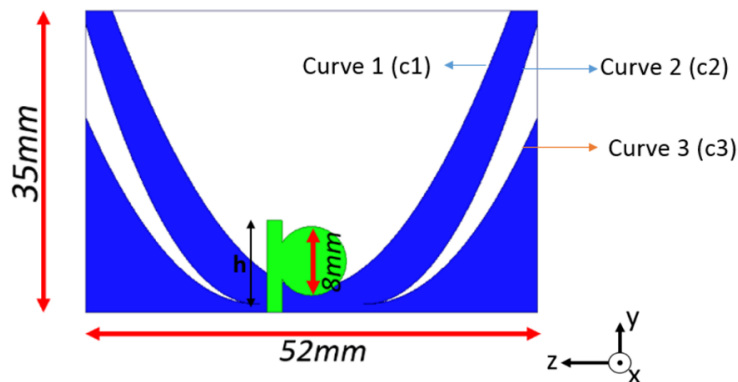

Figure 4.19 : The simulated element antenna.

S11 of the antenna is demonstrated in Figure 4.20 which includes two frequency bands and covers the frequency range between 7-12 GHz.
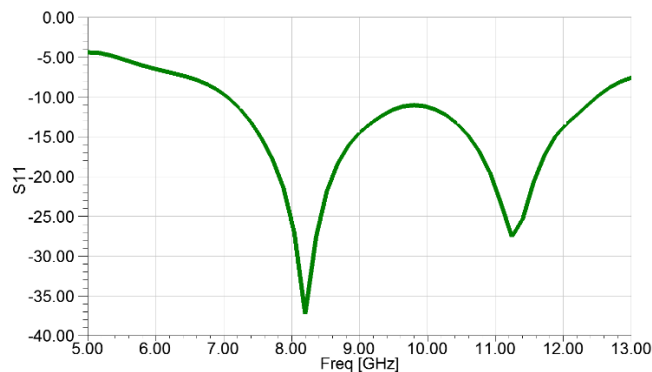

Figure 4.20 : S11 of the element antenna.

37

The antenna is optimized in a way that its second band is tuned to the desired band between 10-12 GHz. It's due to fact that, direction of the current on the circular patch in the second band causes to a more symmetric beam.

In Figure 4.21, surface currents on the circular patch are demonstrated both for fundamental mode at the frequency of 8.2GHz (Figure 4.21a) and in the higher mode at the frequency of 11.5GHz (Figure 4.21b).
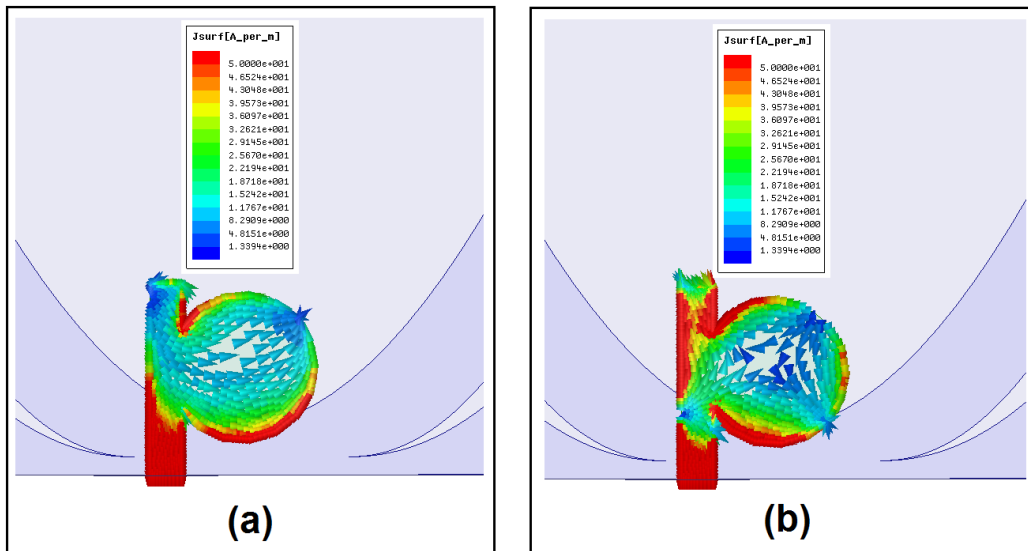
Figure 4.21 : Surface currents on the circular patch (a) frequency of 8.2GHz, (b) frequency of 11.5GHz.

Considering Figure 4.21, it can be clearly clarified that different edges of the circular patch cause to the resonance at the two frequencies of 8.2GHz and 11.5GHz. Validity of this issue can be simply confirmed by considering the intensity of electric fields on the circular patch demonstrated in Figure 4.22. In comparison with Figure 4.22a (8.2GHz), position of the radiating edges of the circular patch in Figure 4.22b (11.5GHz) are more symmetric with respect to the ground plane. Consequently, it is expected to have a more symmetric pattern in the frequency of 11.5GHz compared to 8.2GHz.

It is clearly demonstrated that electric fields on the ground plane in Figure 4.23b (11.5 GHz) is in a very symmetric form on the both sides and positions. This is the main accomplishment made by firstly appropriate feed leading to conduct the surface currents in the desired direction, and subsequently selecting the proper band. But, the electric fields on the ground plane in Figure 4.23a (8.2GHz) is not in a symmetric form, and consequently causes to an asymmetric radiation.
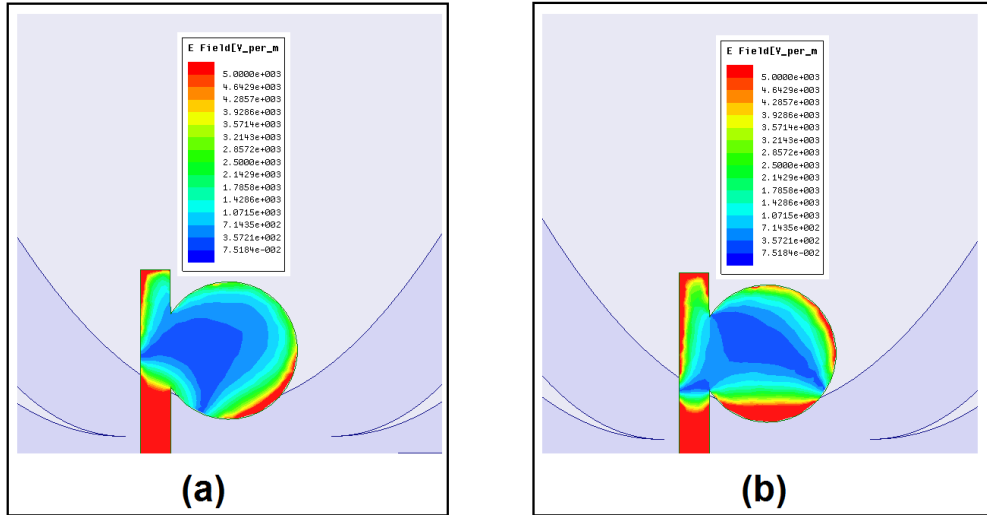
Figure 4.22 : Electric fields on the circular patch (a) frequency of 8.2GHz, (b) frequency of 11.5GHz.
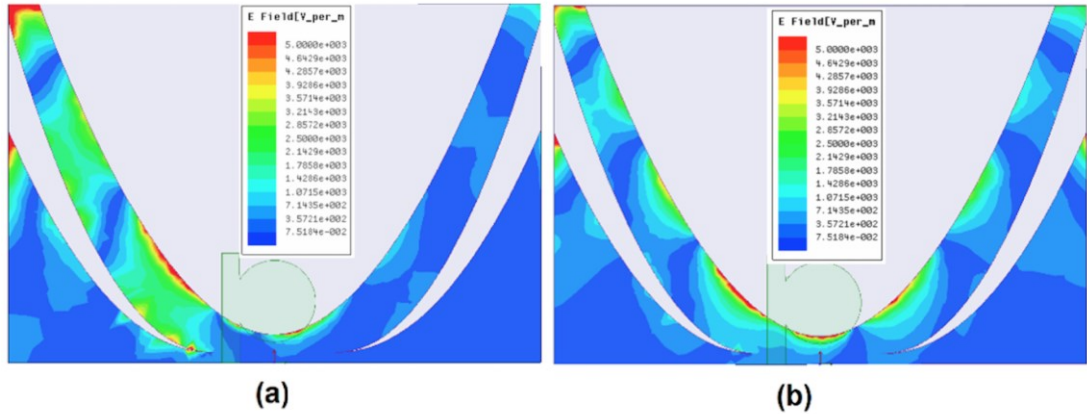
Figure 4.23 : Intensity of electric fields on the parabolic ground,(a) frequency of 8.2GHz, (b) frequency of 11.5GHz.

Figure 4.24 clearly confirms the results observed in Figures 4.21, 4.22 and 4.23 by demonstrating the symmetry of electric fields in the substrate layer. In comparison with Figure 4.24a (8.2GHz), intensity of the electric fields in the substrate layer is in a very symmetric form in Figure 4.24b.

It is clarified that this symmetry observed in Figures 4.23 and 4.24 is the result of the characteristics observed in Figures 4.21 and 4.22 made by the appropriate feeding and selecting the proper band. In fact, the major parameters determining the appropriate surface current in Figure 4.21 are dimensions and position of the feed line beside the circular patch. For instance, compared to the beam of the optimized antenna with $h = 10.7mm$, the beam of antenna with $h = 9.5\ mm$ is asymmetrically deformed. Although,

effect of parameter c_1 (same as c_2 and c_3) on beam of the antenna is also shown in Figure 4.25.
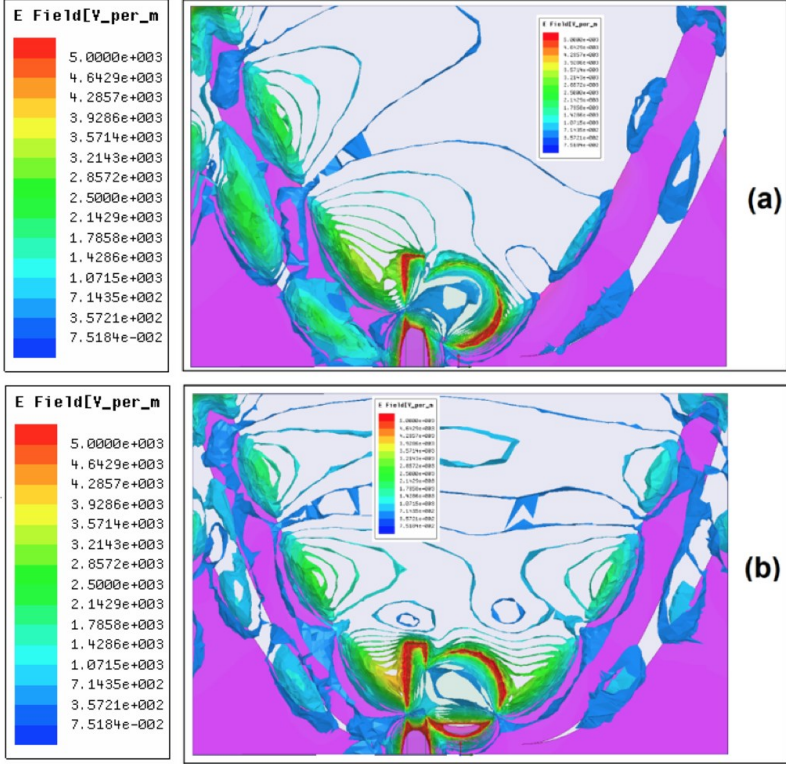
Figure 4.24 : Intensity of electric fields in the substrate layer(a) frequency of 8.2GHz, (b) frequency of 11.5GHz.
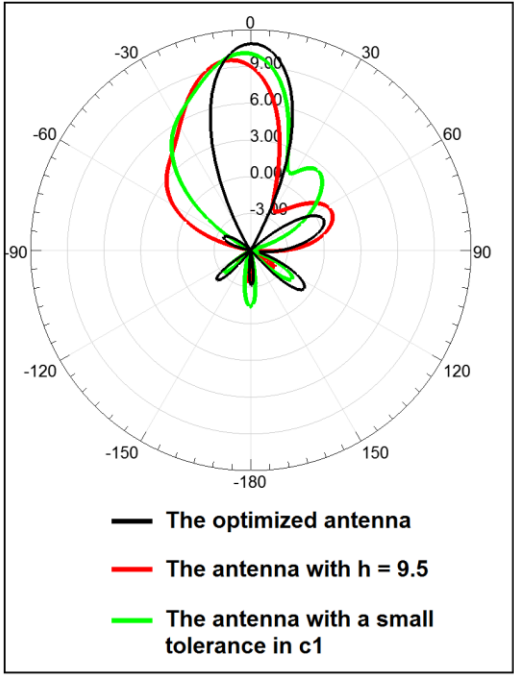
Figure 4.25 : Effects of h and c1 on beam of the antenna at the frequency of 11.5 GHz.

Finally, Figure 4.26 confirms the results shown in Figures 4.21-4.24 by comparing symmetry of beams of the antenna at the two frequencies of 8.2 GHz and 11.5 GHz.
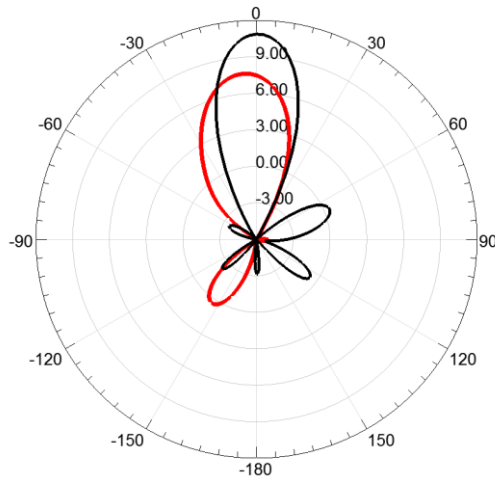
Figure 4.26 : Beam of the antenna at the two frequencies of 8.2GHz and 11.5GHz.

Although, the symmetrical and directive beam in the frequency of 11.5GHz is achieved to use for array design with 2λ spacing. However, the beam at the frequency of 8.2 GHz is desired enough for use to array design around λ spacing. Then, the designed array can be used as a double band array for both the frequencies of 11.5GHz and 8.2GHz by using a double band or wide band feed network.

Finally, beams of the antenna are demonstrated in Figure 4.27 in both E-plane and H-plane.
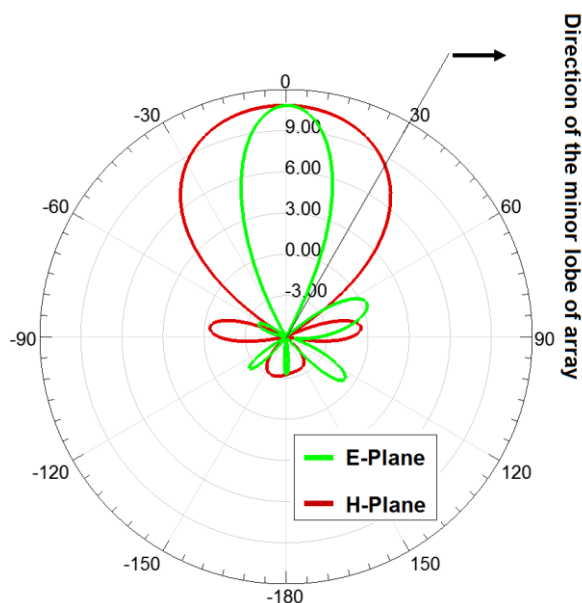
Figure 4.27 : Beams of the antenna in E-plane and H-plane.

41

Normalized intensity of the beam in E-plane in 30 degrees from the maximum pointing direction is -16dB. This is the direction in which the minor lobe would be placed in the array with 2λ spacing (the black line in Figure 4.27). Therefore, that normalized -16dB value in the beam of the element antenna is low enough to cancel the minor lobes of the array factor. Thus, the broadside array with 2λ spacing is designed corresponding to that beam in E-plane.

Also, beams of the antenna in both E-plane and H-plane for both Co-Polarization and Cross-Polarization are demonstrated in Figure 4.28. Considering the position of antenna in Figure 4.19, E-plane of the antenna is in *z-y* plane and H-plane is in *x-y* plane.
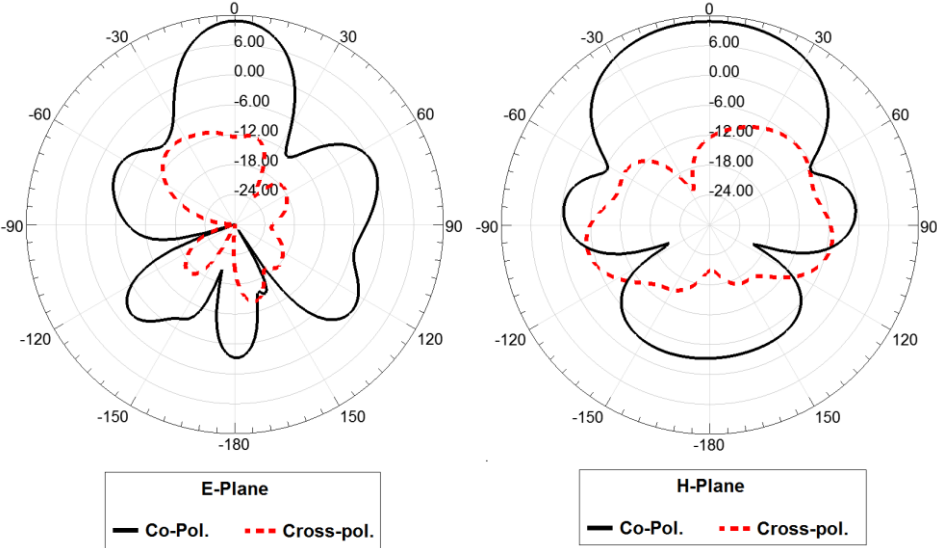
Figure 4.28 : Beams of the antenna in E-plane and H-plane and for Co-Polarization and Cross-Polarization.

Input impedance of the simulated wave-port and that of the antenna with its real and imaginal parts are demonstrated in Figure 4.29.
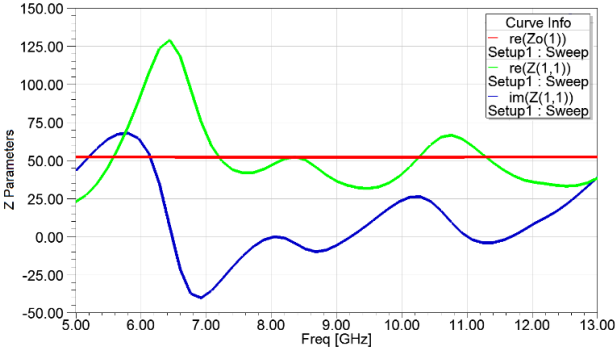
Figure 4.29 : Input impedance of the simulated wave-port and that of the antenna.

The prototype antenna is fabricated and shown in Figure 4.30.

Figure 4.30 : Prototype of the antenna.

Simulated and measured S11 of the the antenna are compared to each other in Figure 4.31. In high frequency operations such as this design, S11 parameter is very sensitive to the accuracy of the soldering and connecting segment between the antenna and SMA connector. Also, a negligible variety in the relative permittivity of the substrate changes the results. Although, in frequency of 8.2GHz both the measurements confirm the simulation results. But, sensitivity of the design to the soldering is seen in Figure 4.31 for more than 10dB difference in 8.2 GHz between S11 parameters of those element antennas in right and left sides of Figure 4.30. This is a deforming factor mostly in the higher frequency of 11.5GHz which made a considerable undesirable effect on S11 parameter. However, it is clarified in the following that the soldering and mounting the SMA connector is performed correctly for the array structure after two tries.
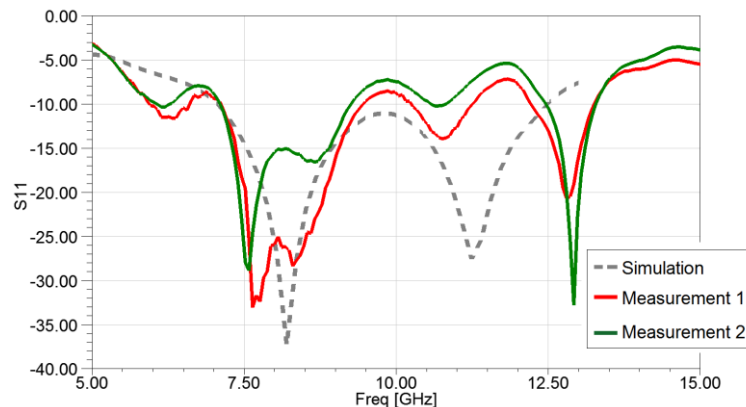
Figure 4.31 : Comparison between the simulated and measured S11.

4.4.2 Array simulation and measurement results

In Figure 4.27, beam of the antenna is very directive at E-plane with two nulls at 30 degrees from the direction of the maximum in the beam. Therefore, the array factor

with 2λ element spacing having two minor lobes at θ = 30 and θ = 120 degrees is used to design the array antenna.

The designed feed network with its dimensions is demonstrated 4.32. In the design with λ spacing, the feed network includes 16 power splitters. However, it is seen in Figure 4.32 that the number of power splitters is reduced to 7. This is the major achievement of this design causing to reduce the loss. The input port is named as port 1 and the output ports are named as port 2- port 9. In any stage of the feed network a simple 1(50 ohm) to 2(100 ohm) power divider is used, where, impedance of any output port is transformed from 100ohm to 50 ohm, by using a 70.71 ohm of a λ/4 transformer. Width of the lines are calculated considering the properties of the substrate in 11.5GHz and the lengths are shown in Figure 4.32.
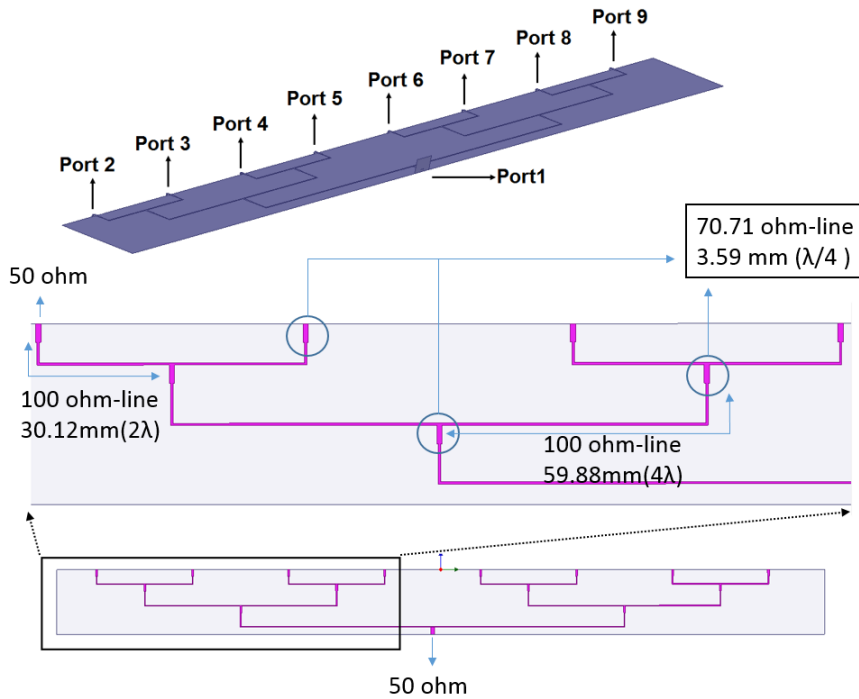
Figure 4.32 : Feed network of the 8-element array.

In order to better observe behavior of the feed network, S parameters are demonstrated. Figure 4.33 demonstrates the S11-S99 of the ports. The input port is matched in a wide range, however the output ports are matched in a narrow band. This drawback is due to low isolation between the output ports made by using standard power dividers.

Also, the S21-S91 parameters in Figure 4.34 demonstrate the ratio of transmitted power to the output ports which is around -11dB.
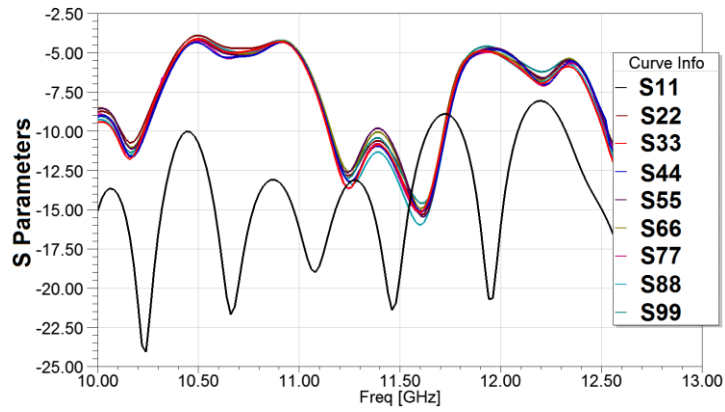
Figure 4.33 : S11-S99 parameters of the feed network.
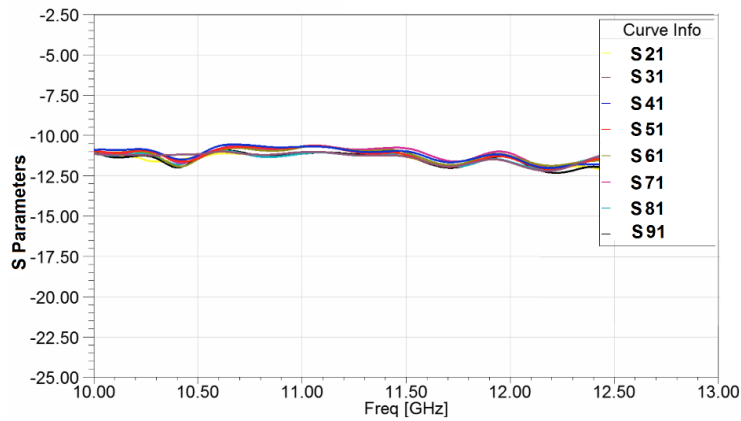
Figure 4.34 : S21-S91 parameters of the feed network.

In Figure 4.35, isolation parameters (S23, S24 and S26) of the feed network are demonstrated.
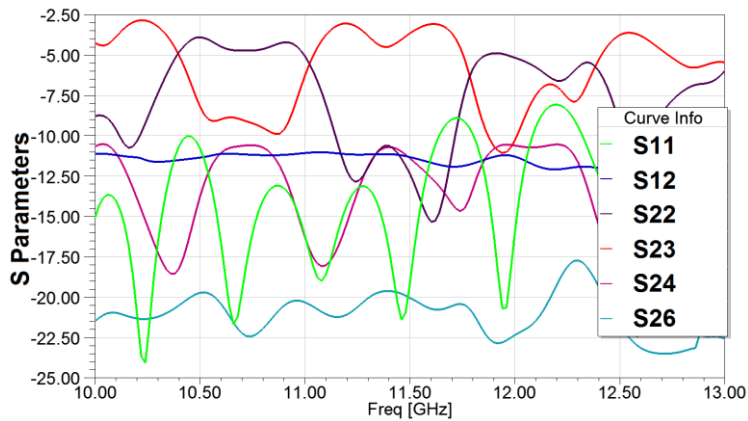
Figure 4.35 : S11, S12, S22, S23, S24 and S26 of the feed network.

It is seen that, the S23 which describes the isolation between port 2 and port 3 is undesirably high. However, this result is more undesirable in phased arrays where

signals with different phases must be collected, and is not disturbing in the application of this design using a fixed beam towards the broadside.

Then, the 8-element array antenna with 2λ spacing is simulated and shown in Figure 4.36.
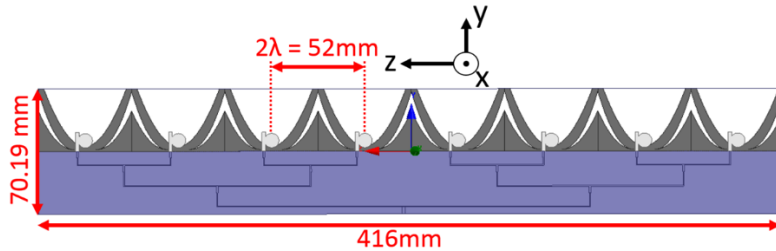
Figure 4.36 : The 8-element array antenna.

Input impedance of the simulated wave-port and that of the antenna with its real and imaginal parts are demonstrated in Figure 4.37.
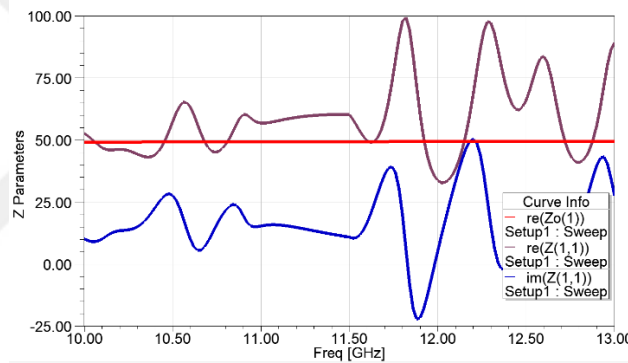
Figure 4.37 : Input impedance of the simulated wave-port and that of the antenna.

Then, S11 parameter of the designed array antenna is compared to those of the element antenna and the feed network in Figure 4.38
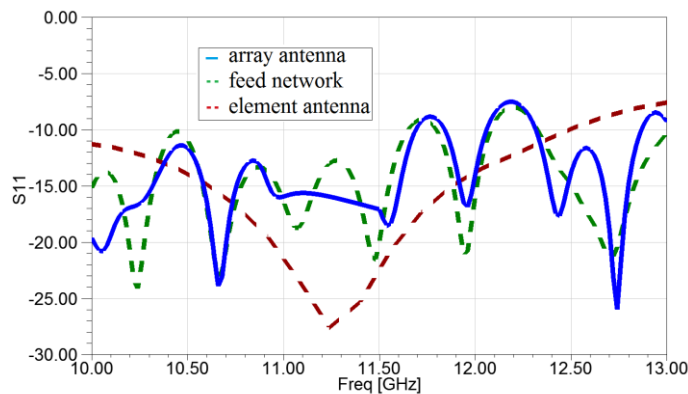
Figure 4.38 : S11 parameters of the designed 8-element antenna compared to the S11 parameters of the element and feed network.

Radiation pattern of the array in E-plane is demonstrated in Figure 4.39. It is seen that the normalized intensity of that side lobe at $\theta = 60°$ is -16 dB which is corresponding to the intensity of the element antenna. However, intensity of the side lobe at $\theta = 120°$ is -12dB. The most important achieve is the very narrow HPBW of the antenna around 3 degrees seen in Figure 4.39 between the two points m_2 and m_3. Also, gain of the antenna reaches to 17.6 dBi.
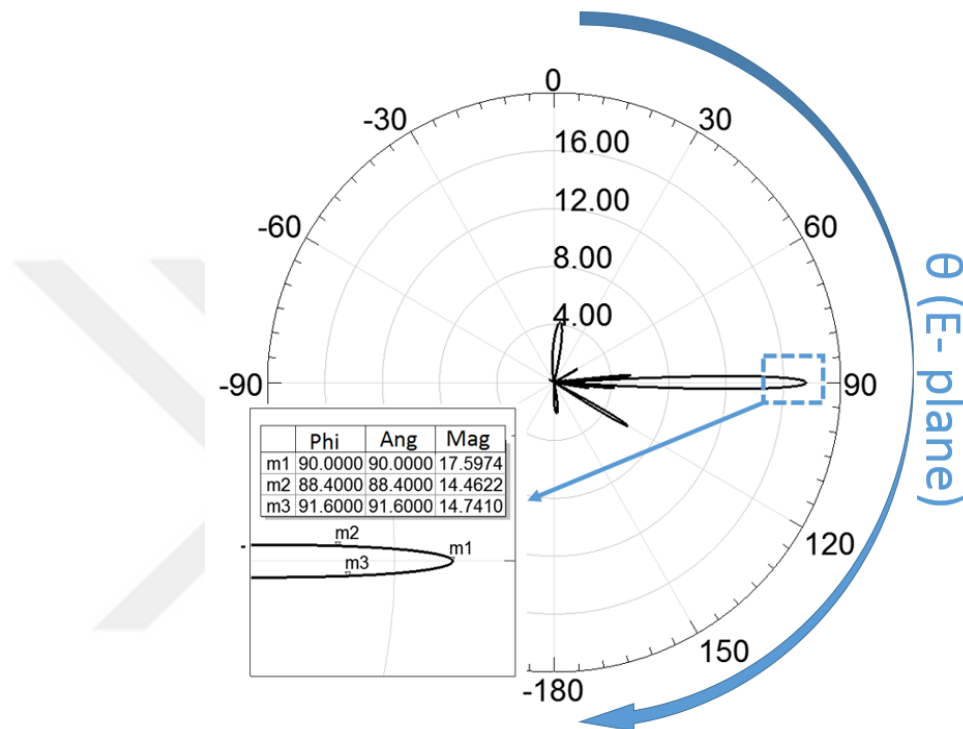
Figure 4.39 : Radiation pattern of the 8-element antenna at the frequency of 11.5 GHz at $\phi = 90°$.

Also, 3D radiation pattern of the array antenna is demonstrated in Figure 4.40 from different views. Beam of the antenna in H-plane is not directional due to fact that the array is established in E-plane. Also, beside those side lobes observed in Figure 4.39 at $\theta = 60°$ and at $\theta = 120°$ in $\varphi = 90°$ plane, other sidelobes within $0° < \theta < 60°$ and $120° < \theta < 180°$ at beyond the $\varphi = 90°$ plane (even out of $60° < \varphi < 120°$) are obserbed. It must be noted that this array antenna is designed to be used as a receiver in geosynchronic satellite system, where it is required and enough to use a very directional beam in one plane. Therefore, the beam in H-plane and those side lobes beyond the $\varphi = 90°$ are not disturbing. However, in the following section these side lobes are cancelled by using another array (nonlinear) in H-plane.
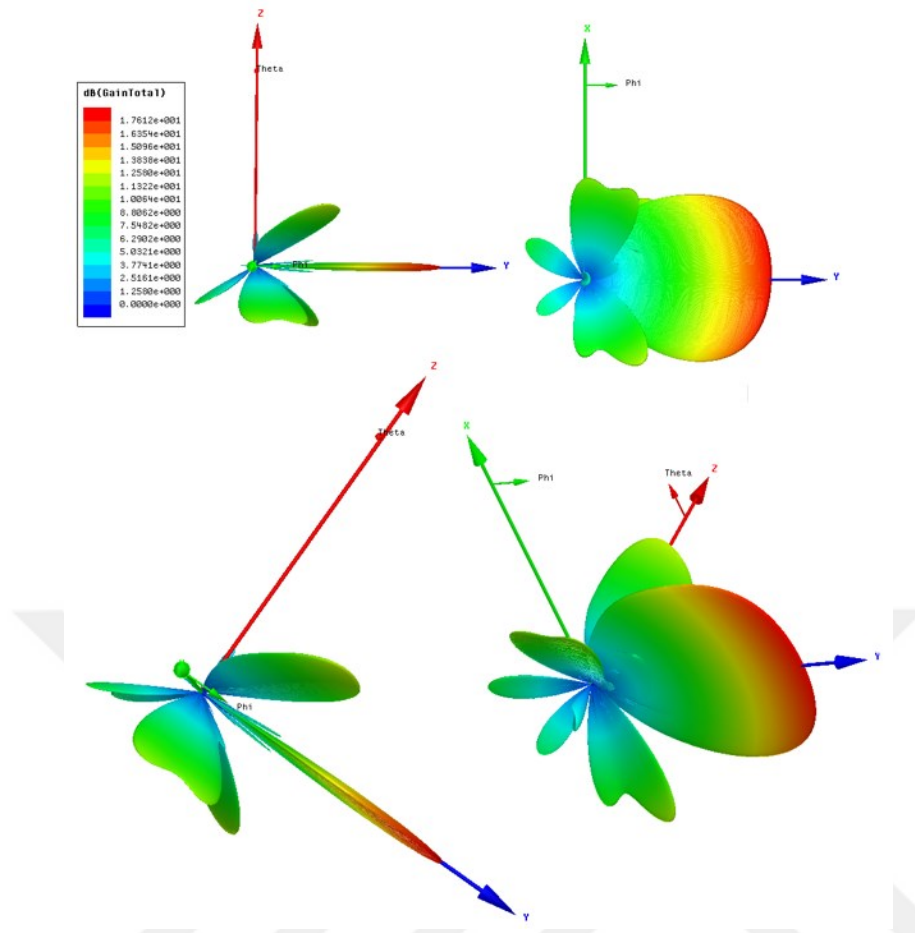
Figure 4.40 : 3D Radiation pattern of the 8-element antenna at the frequency of 11.5 GHz.

The prototype antennas are fabricated and measured. In Figure 4.41 two sides of the fabricated 8-element array antenna is demonstrated. However, due to sensitivity of the design to the soldering section, wrongly mounting SMA connector and using a very short feed line in the arrival of the first divider, the S parameters did not confirm the simulation results.
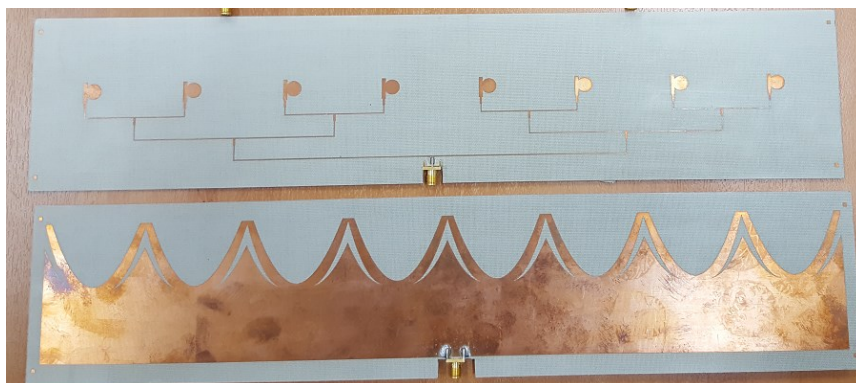
Figure 4.41 : First prototype of the array antenna.

Then, the second 4-element antenna is fabricated by using a long feed line and correctly mounting (and soldering) the SMA connector as in Figure 4.42.
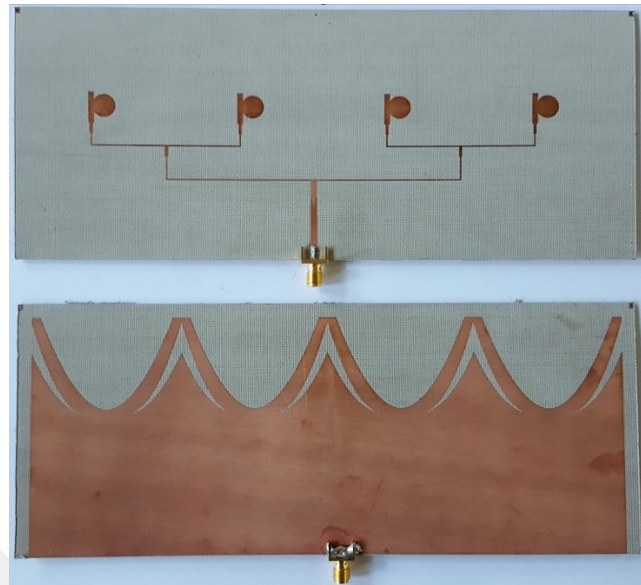
Figure 4.42 : Second prototype of the array antenna.

Consequently, the measured S11 parameter desirably confirmed the simulation results particularly in the range of 10-12 GHz as demonstrated in Figure 4.43. It was not possible to continue the process of fabrication and measurement again for 8-element array due to some restrictions. However, the measurements of radiation pattern provided in the following for the 4-element array confirm the accuracy of the method for array with 8 or any number of elements.
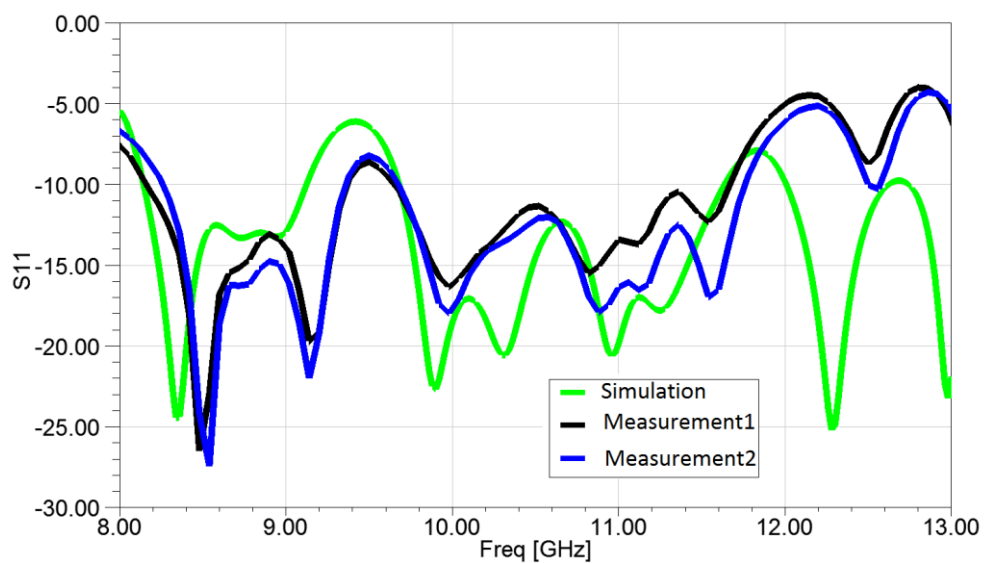
Figure 4.43 : Measured and simulated S11 parameter of the antenna.

Radiation pattern of the 4-element array antenna is measured in the two perpendicular planes (E-plane and H-plane). The radiation pattern is measured at several frequencies in the range of 10-12 GHz and the measured results desirably confirmed the simulated results. However, only the measurements in 11.5 GHz are demonstrated to confirm the simulated radiation patterns which are provided in the frequency of 11.5 GHz. The Antenna Under Test (AUT) was placed in 1 meter away from the reference antenna which was a pyramidal horn antenna to meet the requirement of far field measurement setup that is $2\frac{D^2}{\lambda}$ (in which D is the largest dimension of the antenna that is 21 cm for the 4-element array)[27] considering the frequency of operation that is 11.5GHz. Both the antennas are placed along the line of sight direction of each other with conformity of polarization direction. Finally, the AUT is rotated with respect to the reference antenna by using a turntable. The achieved results are provided in Figures 4.44, 4.45 and 4.46.

In Figure 4.44, the measured and simulated radiation patterns are compared with each other at 11.5 GHz throughout the $0° \ll \theta \ll 180°$ in E-plane ($\phi = 90°$, z-y plane) of the antenna.

Figure 4.44 : Simulated and measured radiation patterns of the 4-element array in E-plane at the frequency of 11.5 GHz in $\phi = 90°$ through $0° \ll \theta \ll 180°$.

As it is seen in Figure 4.44, the measured beam desirably confirm the simulated beam particularly in the ranges of main lobe and its adjacent side lobes. The main lobe around $\theta = 90°$ degrees desirably conform that of the simulated pattern. Also,

neglecting the nuls of the beam and small variations and shifts, the measured beam follows and conforms the simulated pattern along the 0° ≪ θ ≪ 180°. However, the beam in E-plane is measured again in the smaller range of 60° ≪ θ ≪ 120° and is demonstrated in Figure 4.45.
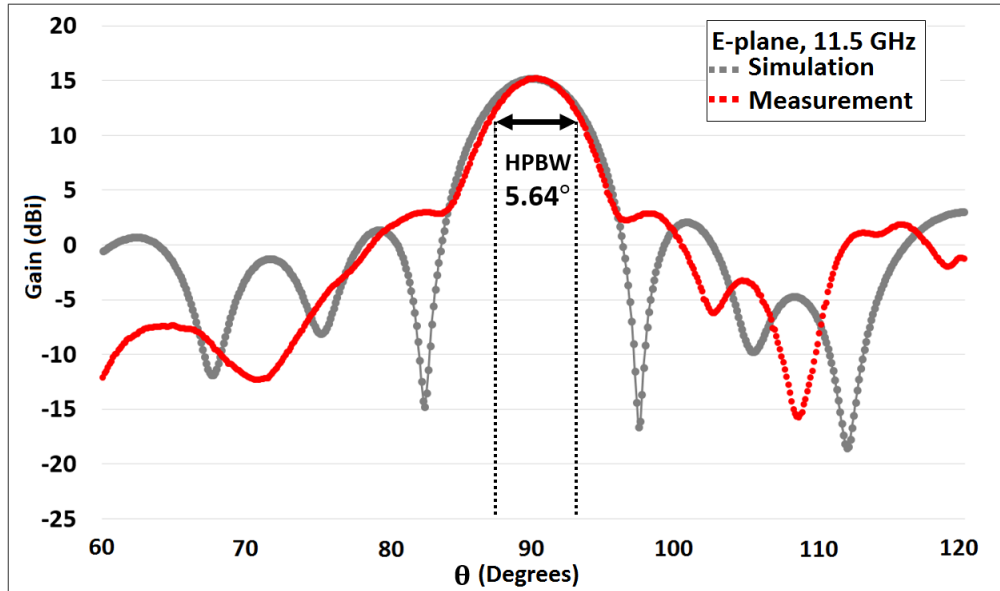
Figure 4.45 : Simulated and measured radiation patterns of the 4-element array in E-plane at the frequency of 11.5 GHz in $\phi = 90°$ through $60° \ll \theta \ll 120°$.

In figure 4.45, the measured values along the main lobe at E-plane and 11.5 GHz again confirm the simulated beam. The measured value of HPBW is 5.64° that is satisfactory comparing to the simulated value of 6.2° and confirm the expected results for the 4-element antenna. The observed gain of the antenna in both of the measurements is 15.2 dBi. Also, intensity of the first side lobes are -12.5 dB less than the intensity of main lobe as seen in both the Figure 4.44 and Figure 4.45 that confirm the expected values for the 4-element array. However, this value should be optimized as low as -25 dBi for practical long range satellite applications by using larger arrays. Intensity of the side lobes at $\theta = 60°$ and $\theta = 120°$ are also at least -14 dB (with a little shift) less than the intensity of the main lobe that confirms the intended goals in this design method in which the number of elements are reduced (by using 2λ spacing). It must be noted that, amplitude of those side lobes (which are in the direction of the second strong lobes next to the main lobe in array factor with 2λ spacing) would be as strong as the main lobe without using the very directive element antenna. The amount of 5.64° HPBW that is achieved by the 4-element array can be reached only by using eight lements by the conventional method with λ spacing. Finally, the obtained results of the

4-element antenna (the achieved 5.64° for HPBW and the desirable levels for the first side lobes and those at 60° and 120°) confirm the availability of achieving the same desirable results for the 8-element array (with 2λ spacing) and subsequently, confirm the validity of the calculations in Section 4.2.

Radiation pattern at the same frequency 11.5 GHz is measured in H-plane ($\theta = 90°$, x-y plane) of the antenna that is demonstrated in Figure 4.46.
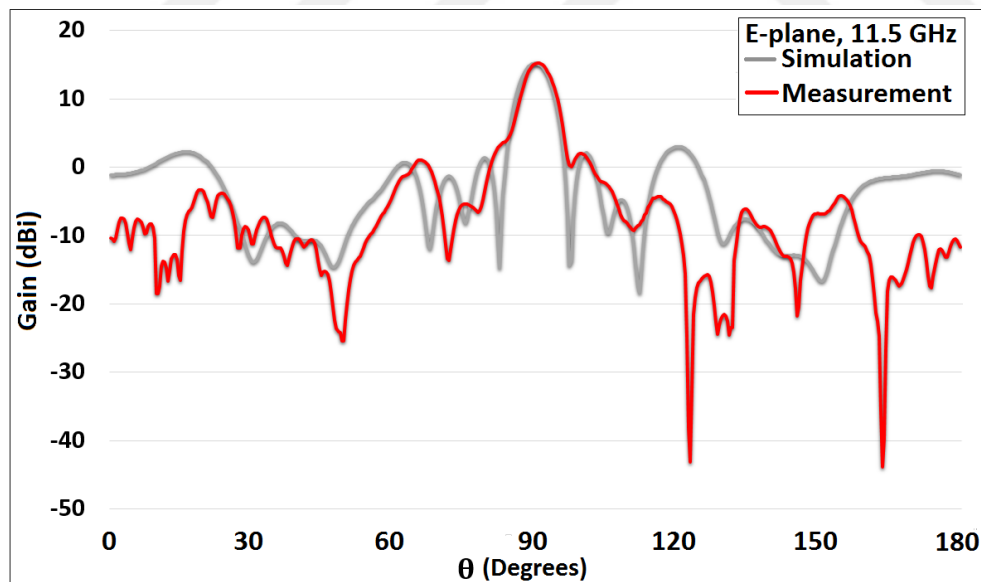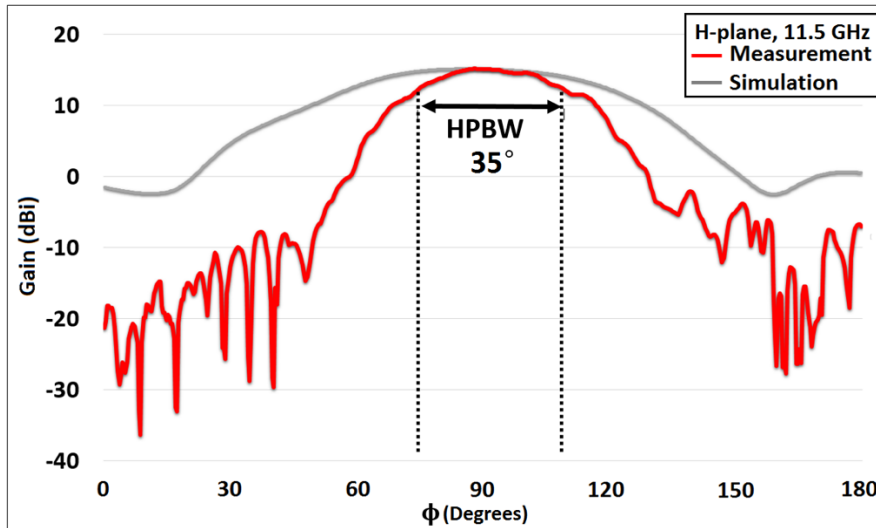

Figure 4.46 : Simulated and measured radiation patterns of the 4-element array in H-plane at the frequency of 11.5 GHz in $\theta = 90°$ through $0° \ll \phi \ll 180°$.

The measured beam in Figure 4.46 demonstrates better performance compared to the simulated beam in H-plane. HPBW value of the antenna in H-plane reach to 35°. Although, forms of the beams are very similar however, a difference is seen in Figure 4.46 that is increasing regularly towards $\phi = 0°$ and $\phi = 180°$. Also, the nulls in the simulations are not observed in the measured results in E-plane in Figure 4.44 and Figure 4.45. Along with, Figure 4.44 demonstrates a little shift in the position of the side lobes. Although, the measurement is performed considering the far field distance requirements however, it must be accomplished by using a larger distance than 1 mm to precisely provide equally phased arrival waves through the aperture of the receiver antenna as is demonstrated in Figure 4.47. There is $\Delta r \approx 0.38\ cm$ variance between the transmission distance of the two arrival waves with 0° and 5° angles of incidence along the aperture of the receiver antenna that makes more than 50° phase difference considering the wavelength ($\frac{\Delta r}{\lambda} \approx 15\%$ for the two waves with 5° difference in angle

of arival at 11.5 GHz and in 1 meter). Then, those minor differences between the simulated and measured patterns are due to the accomplishment of the measurements in a small distance.
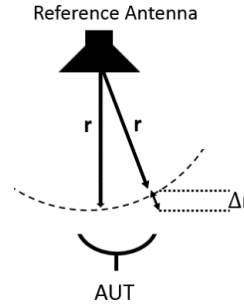
Figure 4.47 : Phase difference between the arrival waves in the aperture of the receiver antenna.

The achieved values observed in Figures 4.44-4.46 are demonstrated in the Table 4.5.

Table 4.5 : Characteristics of the beams in Figures 4.44-4.46.

Characteristics of the beams	Simulated E-plane	Measured E-plane	Simulated H-plane	Measured H-plane
Gain (dBi)	15.2	15.2	15.2	15.2
HPBW (degrees)	6.2	5.64	60	35
Ratio of the first side lobe to main lobe (dB)	-13	-12.5	-15	-22
Ratio of the side lobes in 30° next to main lobe (dB)	-14 for $\theta = 60°$ -12 for $\theta = 120°$	-22 for $\theta = 60°$ -13 for $\theta = 120°$	-	-

It is observed that the isolation between the outputs ports of the standard feed network used in the design is considerably high. Though, it is noted that it is not important for the aim of this thesis. However, the array is also simulated based on the Wilkinson feeding network. But, it is not fabricated due to the high fabrication costs and also high losses in the Wilkinson dividers. The simulated structure is shown in Figure 4.48 with its dimensions and properties.

Also, S parameters of the feed network based on Wilkinson divider are compared to those of the standard feed network in Figure 4.49.
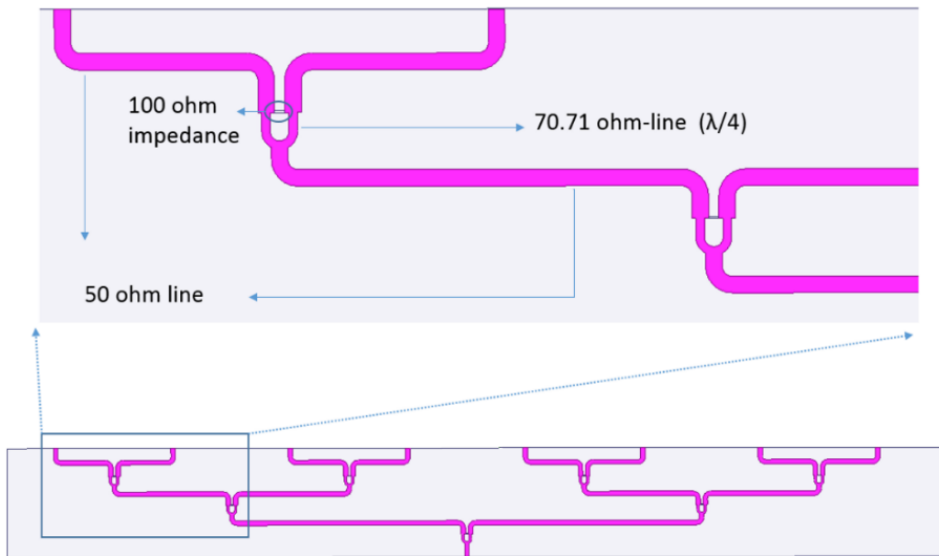
Figure 4.48 : Wilkinson feed network at the frequency of 11.5GHz.
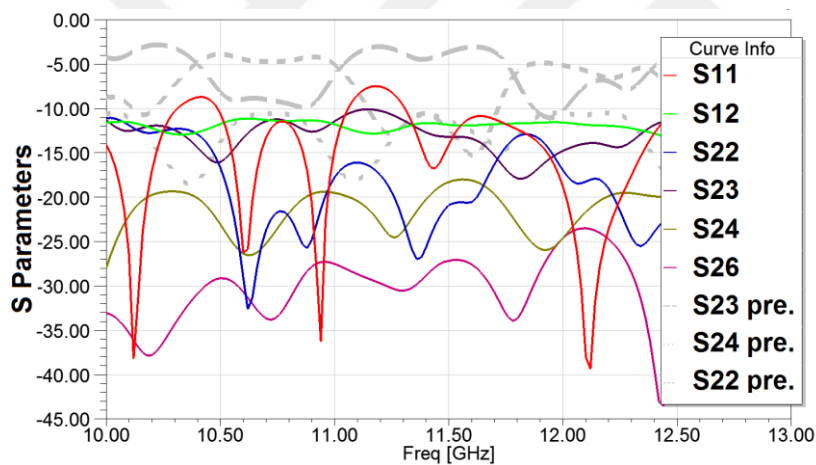
Figure 4.49 : Comparison between the S parameters of Standard and Wilkinson feed network.

Then, the antenna is also designed based the Wilkinson feed network and is shown in Figure 4.50. Also, S11 parameters of the antennas with standard and Wilkinson based feed network are compared to each other in Figure 4.51.
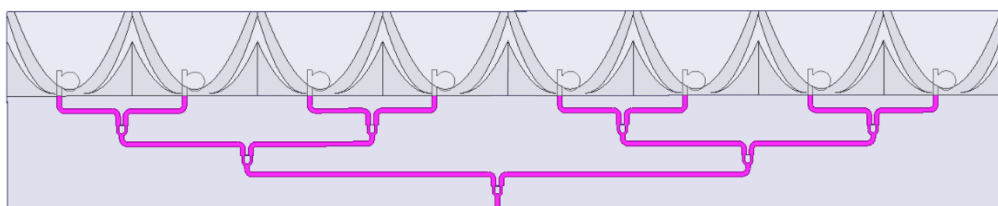
Figure 4.50 : Designed antenna based on Wilkinson feed network.

54
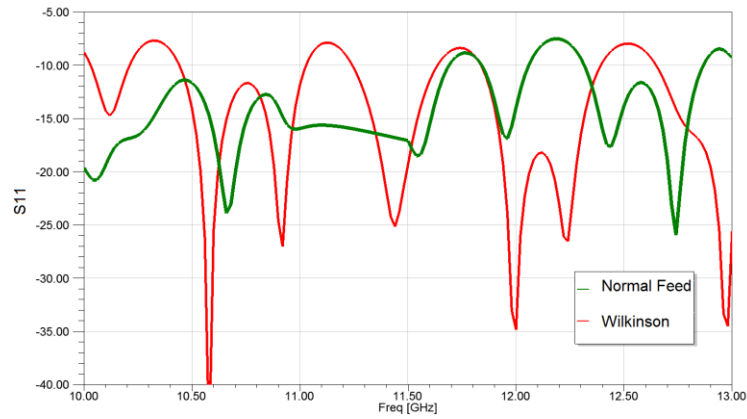
Figure 4.51 : Comparison between the S11 parameters of antennas with standard and Wilkinson based feed network.

Beam of the element antenna presented in Figure 4.19 in H-plane is not as directive as the beam in the E-plane to design a planar array with 2λ spacing between all the elements. However, linear array of that array antenna shown in Figure 4.36 (8-element array) with λ spacing is developed in H-plane (y-x plane), resulting in a planar array such as that demonstrated in Figure 2.2. Simulated radiation pattern of the planar array antenna is demonstrated in Figure 4.52. Gain of the antenna reachs to 28dBi. Also, the large side lobes seen in Figure 4.40 are canceled by using this planar configuration.
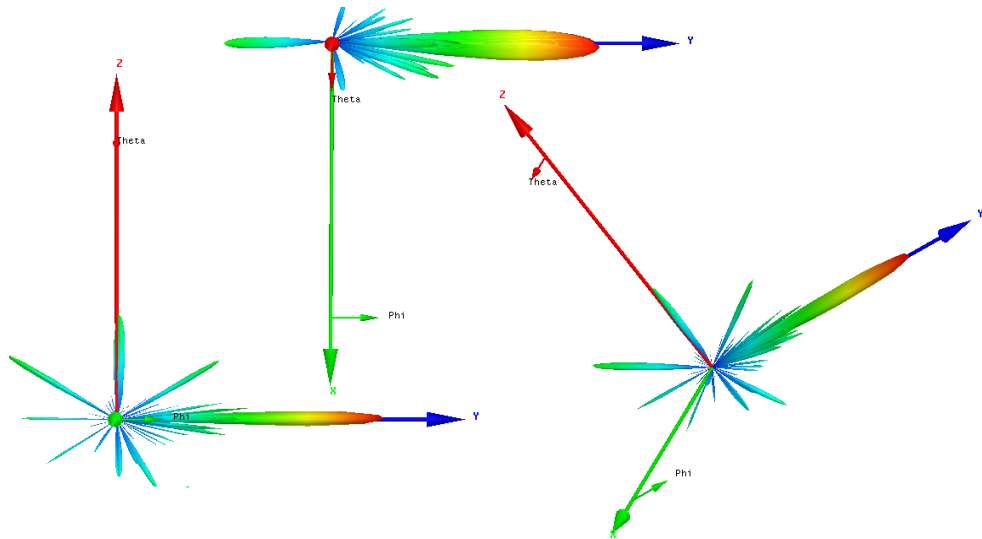
Figure 4.52 : 3D beams of the planar 8×8-array antenna.

Then, a planar array is developed based on the nonlinear array of the 8-element antenna in (y-z) plane by using the results of Section 4.3. The planar array antenna is demonstrated in Figure 4.53 in which the 8-element antennas (designed with 2λ spacing) are arranged in the nonlinear form with d_1 and d_2 Spacing's.
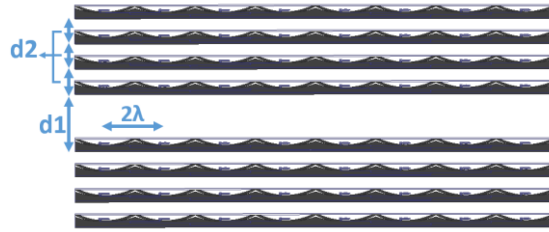
Figure 4.53 : The 8×8 planar array antenna (nonlinear array of the 8-element array antenna).

Main lobe of the beam of that nonlinear array is compared to that of the linear array and demonstrated in Figure 4.54.

Name	Phi	Ang	Mag
m1	90.0000	90.0000	27.3291
m2	90.0000	90.0000	26.6634
m3	87.0000	87.0000	23.7849
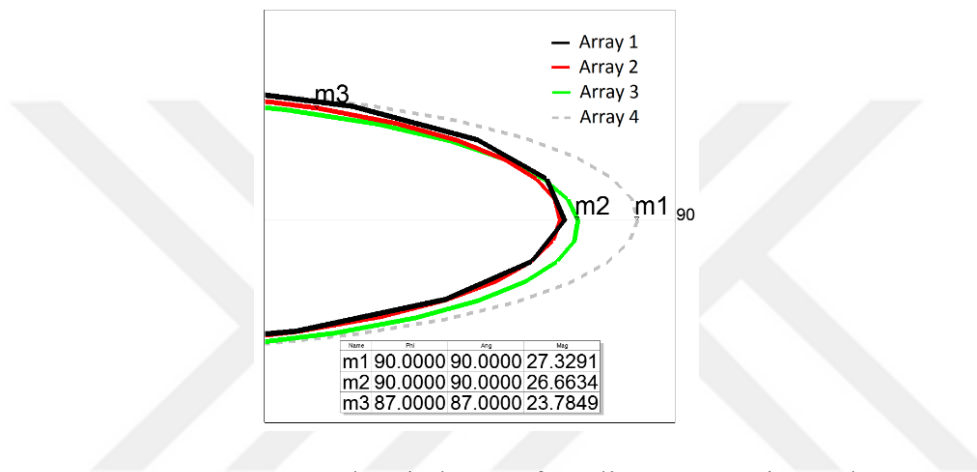
Figure 4.54 : Compared main beam of nonlinear arrays in H-plane.

In this Figure, array1 is the 8×8-planar array (linear array of the 8-element array) with 26mm (λ) spacing. Array 2 is 8×8 planar array (nonlinear array of the 8-element array) with d_1 = 38mm and d_2 = 24mm spacing's and array3 is with d_1 = 50mm and d_2 = 22mm spacing's. Parameters d_1 and d_2 are defined in Figure 4.13. It should be noted that the simulations' analysis are performed up to limited steps (due to the limitation of the computer memory where number of meshes in the simulation reached over 1 million) to only demonstrate the effect of nonlinear design on the beam. However, simulation results of array2 and array3 demonstrated narrower beam compared to array1, as seen in Figure 4.54, that is the aim of the nonlinear method proposed in Section 4.3. Points m_1, m_2 and m_3 are mentioned in Figure 4.54 as measures of HPBW of array1 and comparison between the HPBW of the beams. Array 4 demonstrates the beam of array 3 with one more step of analyses accuracy in simulations. The amount of improvement in Figure 4.54 may be seen small due to fact that d_2 is selected in a range having smaller deformed effect on side lobes and the improvement will be increased by more reduce of d_2.

5. CALCULATION OF A COMPACT EXPRESSION FOR THE ARRAY FACTOR AND DIRECTIVITY OF BINOMIAL ARRAY WITH NO RESTRICTION ON ELEMENT SPACING

5.1 Introduction

Antenna arrays possess several capabilities, such as fast electronic beam steering, reconfigurability, conformal characteristics and adaptive pattern reshaping [23]. Configurability of the beam of array antennas is their most favorite property. In some array structures such as smart array antennas, the beam of array antenna can be formed in order to achieve preferred aims such as low SLL. In many of the practical applications, such as in radar, imaging or satellite communications [22], it is required to reduce the SLL of the radiation pattern of an antenna array [18,19] to minimize interference from unwanted sources (or the interference made by adjacent satellites in satellite communication)[20].

Several designs have been proposed to reduce the SLL of array antennas. The most favorite approaches are the use of Genetic Algorithms (GA) as in [24-26]. However, most of the designs lead to a limited level of improvement in SLL. Binomial arrays with the element spacing equal or less than $\lambda/2$ have no minor lobes [27].

In general, Binomial arrays demonstrate the most favorite property in term of SLL. However, no compact expressions exist for the array factor and directivity for binomial arrays with no restriction in element spacing, except for $\lambda/2$ element spacing [27,55].

In this section, a formal procedure is proposed to derive compact expressions for the array factor and directivity of binomial arrays. The properties of Pascal's triangle, upon which the excitation coefficients of the binomial array are based and distributed, are used to obtain the compact expressions.

It is demonstrated that the excitation coefficients of an N-element binomial array can be expressed as an (N-2)th convolution of the two-element binomial array. Then, the array factor and directivity of the entire binomial array is obtained using the properties of Fourier transform.

5.2 Properties of Pascal's Triangle and the Excitation Coefficients of the Binomial Array

In this section, a formal procedure is outlined to derive compact expressions for the array factor and directivity of the binomial array, with no restriction in element spacing and number of elements.

The excitation coefficients for the binomial array are distributed by a series using the binomial expansion presented in [27,56]. The coefficients of the series expansion for different values of N can be demonstrated by using Pascal's triangle, as in Figure 5.1 for 6 elements (up to 10 elements in [27]). The elements in Figure 5.1 are uniformly spaced with d spacing along the z axis. While d is the total separation between the elements, another separation s is introduced as in Figure 5.1 ($s = d/2$), to conveniently illustrate the derivation; $z = 0$ represents the physical center of the array.
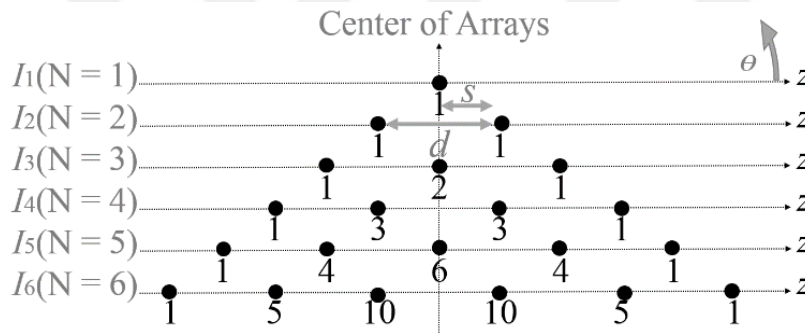
Figure 5.1 : Distribution of the excitation coefficients for binomial arrays in the form of Pascal's triangle up to 6 elements along z axis.

Assume that all the elements are fed without a progressive phase shift. Then, the excitation distributions for the binomial array composed of different number of elements can be written as listed on Table 5.1.

Table 5.1 : Amplitude excitation distribution for the binomial arrays composed of different number of elements.

Number of elements	Array amplitude excitation distribution
	$[\delta(z \pm s) = \delta(z + s) + \delta(z - s)]$
N = 1	$I_1(z) = \delta(z)$
N = 2	$I_2(z) = \delta(z \pm s)$
N = 3	$I_3(z) = 2\delta(z) + \delta(z \pm 2s)$
N = 4	$I_4(z) = 3\delta(z \pm s) + \delta(z \pm 3s)$
N = 5	$I_5(z) = 6\delta(z) + 4\,\delta(z \pm 2s) + \delta(z \pm 4s)$
N = 6	$I_6(z) = 10\delta(z \pm s) + 5\delta(z \pm 3s) + \delta(z \pm 5s)$

The amplitude excitation coefficients demonstrated by Pascal's triangle in Figure 5.1 exhibit a regular behavior. The most apparent property is that, as the number of elements increases, the amplitude of the central elements increases compared to the amplitudes of the ones at the edges. This behavior, along with its symmetry on both sides of the z axis, is very similar to the properties of the convolution of two symmetric distributions [52]. On the other hand, convolution of two distributions with N_1 and N_2 elements has N_1+N_2-1 elements. Therefore, considering the number of elements in the consecutive rows of the Pascal's triangle (which is regularly increased with one element), the rows in Pascal's triangle are developed by convolving their previous row with another two-element distribution resulting in an increase of only one element. Consequently, taking into account the second row of Pascal's triangle which includes only two elements and convolving ($*$ indicates convolution) its excitation distribution $I_2(z)$, shown in Table 5.1, with the first row $I_1(z)$, as in (5.1)

$$\delta(z \pm s) * I_1(z) = \delta(z \pm s) * \delta(z) = \delta(z \pm s) = I_2(z) \tag{5.1}$$

confirms that the convolution of the excitation distribution of the first row with $\delta(z \pm s)$ results in the second row $I_2(z)$ of the excitation distribution of the binomial array (the procedure for this and the following convolutions is demonstrated in Section 4.2).

Thus, the observed properties in Pascal's triangle are confirmed. Continuing with the second row of Figure 5.1 and convolving the second excitation distribution $I_2(z)$ of Table 5.1 with $\delta(z \pm s)$, as in (5.2), results in the excitation distribution of the third row $I_3(z)$.

$$\delta(z \pm s) * I_2(z) = \delta(z \pm s) * \delta(z \pm s) \tag{5.2}$$
$$= 2\delta(z) + \delta(z \pm 2s) = I_3(z)$$

This procedure is continued for the third, fourth and fifth rows, and it lead to (5.3), (5.4) and (5.5).

$$\delta(z \pm s) * I_3(z) = \delta(z \pm s) * [2\delta(z) + \delta(z \pm 2s)] \tag{5.3}$$
$$= 3\,\delta(z \pm s) + \delta(z \pm 3s) = I_4(z)$$

$$\delta(z \pm s) * I_4(z) = \delta(z \pm s) * [3\,\delta(z \pm s) + \delta(z \pm 3s)] \tag{5.4}$$

$$= 6\delta(z) + 4\,\delta(z \pm 2s) + \delta(z \pm 4s) = I_5(z)$$

$$\delta(z \pm s) * I_5(z) = \delta(z \pm s) * [6\delta(z) + 4\,\delta(z \pm 2s) + \delta(z \pm 4s)] \tag{5.5}$$

$$= 10\,\delta(z \pm s) + 5\,\delta(z \pm 3s) + \delta(z \pm 5s) = I_6(z)$$

In (5.1) - (5.5), it is demonstrated that convolving each of the excitation distributions in rows 1 to 5 of Pascal's triangle with the two-element distribution of the second row $I_2(z) = \delta(z \pm s)$ results in the excitation distribution of their next row of Pascal's triangle.

To demonstrate the procedure, but due to space limitations, only a limited number of convolutions (up to six elements) are provided in (5.1) - (5.5). As a result, the amplitude excitation coefficients of the binomial array with different number of the elements can be written as indicated on Table 5.2.

Table 5.2 : Excitation distribution for the binomial arrays composed of different number of elements.

Number of elements	Array amplitude excitation distribution
N = 1	$I_1(z) = \delta(z)$
N = 2	$I_2(z) = \delta(z \pm s)$
N = 3	$I_3(z) = I_2(z) * I_2(z)$
N = 4	$I_4(z) = I_2(z) * I_2(z) * I_2(z)$
N = 5	$I_5(z) = I_2(z) * I_2(z) * I_2(z) * I_2(z)$
N = 6	$I_6(z) = I_2(z) * I_2(z) * I_2(z) * I_2(z) * I_2(z)$

The most significant result which can be derived from Table 5.2 is that the excitation distribution of all the arrays is represented in terms of only the two-element array with $\delta(z \pm s)$ distribution. More clearly, it is confirmed that the higher-order distributions in all the rows of Pascal's triangle can be demonstrated by simple multiplicative factors $I_2(z)$ of the second row of Table 5.2. Therefore, the array factors corresponding to those excitation distributions of binomial arrays can be expressed using only the array factor of the two-element binomial array; it is, due to this basic characteristic, why binomial arrays demonstrate a limited number of minor lobes. This issue is demonstrated in the following section and in Figure 5.3.

5.3 Derivation of the Array Factor and Directivity for the Binomial Array

The normalized array factor of equally spaced N elements with uniform unit excitation, including even elements (N = 2M) or odd elements (N = 2M+1) with reference point at the physical center of the array, can be written as (5.6) [27]

$$AF_N(\theta) = \frac{1}{N} \sum_{n=0}^{(N-1)} e^{j\left[n-\left(\frac{N-1}{2}\right)\right]\psi} \tag{5.6}$$

$$\psi = kd \cos\theta + \beta \tag{5.6a}$$

where k is the wave number, d and β are the spacing and progressive phase shift between the elements, respectively, and θ is the observation angle with respect to the z axis.

Since the binomial array excitation distribution is related to its array factor through a direct Fourier transform [27,53,54], the array factor can be derived through an inverse Fourier transform. To demonstrate this, consider (5.7) in which the placement of discrete elements are distributed as the sum of (δ) functions along the z axis.

$$I_N(z) = \sum_{n=0}^{(N-1)} \delta\left(z - \left[n - \left(\frac{N-1}{2}\right)\right]d\right) \tag{5.7}$$

Consequently, it can be observed that the array factor in (5.6) is formally the inverse Fourier transform of the excitation distribution of (5.7); also (5.7) is the Fourier transform of (5.6). Therefore, if the excitation distribution of an array is represented by a convolution of minor components, its array factor can be demonstrated by multiplication of minor array factors, corresponding to those minor components, using the multiplication and reciprocity properties of the Fourier transform [52].

The two-element binomial array illustrated in Figure 5.1 or Table 5.2 can be considered as a two-element linear array with uniform and unity excitations. Therefore, the respective array factor can be written as (5.8) by using (5.6).

$$AF_{N=2}(\theta) = \cos\left(\frac{1}{2}\psi\right) = \cos\left(\frac{1}{2} kd \cos\theta\right) \tag{5.8}$$

61

From Table 5.2, the excitation distribution for a three-element binomial array can be written as (5.9)

$$I_3(i) = I_2(i) * I_2(i) \tag{5.9}$$

Therefore, from (5.9) and using the multiplication property of the Fourier transform, the array factor for a three-element binomial array can be written as (5.10).

$$AF_{N=3}(\theta) = [AF_{N=2}(\theta)][AF_{N=2}(\theta)] = \left[\cos\left(\frac{1}{2}\psi\right)\right]\left[\cos\left(\frac{1}{2}\psi\right)\right] \tag{5.10}$$

Consequently, the array factor for all the binomial arrays, with 1-6 elements whose excitation distributions are listed in Table 5.2, are tabulated in Table 5.3.

Table 5.3 : Array Factor calculation for the binomial arrays composed of different number of elements demonstrated in Figure 5.1.

Number of elements	Array amplitude excitation distribution
N = 1	$AF_{N=1}(\theta) = 1$
N = 2	$AF_{N=2}(\theta) = \left[\cos\left(\frac{1}{2}\psi\right)\right]$
N = 3	$AF_{N=3}(\theta) = [AF_{N=2}(\theta)]^2 = \left[\cos\left(\frac{1}{2}\psi\right)\right]^2$
N = 4	$AF_{N=4}(\theta) = AF_{N=3}(\theta)\,AF_{N=2}(\theta) = [AF_{N=2}(\theta)]^3$ $= \left[\cos\left(\frac{1}{2}\psi\right)\right]^3$
N = 5	$AF_{N=5}(\theta) = AF_{N=4}(\theta)\,AF_{N=2}(\theta) = [AF_{N=2}(\theta)]^4$ $= \left[\cos\left(\frac{1}{2}\psi\right)\right]^4$
N = 6	$AF_{N=6}(\theta) = AF_{N=5}(\theta)\,AF_{N=2}(\theta) = [AF_{N=2}(\theta)]^5$ $= \left[\cos\left(\frac{1}{2}\psi\right)\right]^5$

The process illustrated for arrays with up to 6 elements can be continued and expanded to derive the array factor for arrays with larger number of elements.

Following such a procedure, the array factor for a general N-element linear binomial array with even or odd elements, can be written as (5.11).

$$AF_N(\theta) = [AF_{N-1}(\theta)][AF_2(\theta)] = AF_2^{N-1}(\theta) \tag{5.11}$$

$$= \left[\cos\left(\frac{1}{2}\psi\right)\right]^{N-1} = \left[\cos\left(\frac{1}{2}\,kd\cos\theta\right)\right]^{N-1}$$

From [27], the radiation intensity $U(\theta)$ of corresponding array factor can be written as (5.12).

$$U(\theta) = [AF_N(\theta)]^2 = \left[\cos\left(\frac{1}{2}\,kd\cos\theta\right)\right]^{2N-2} \tag{5.12}$$

Based on (5.12), its maximum value (U_{max}) occurs for $\theta = \pi/2$ and it is unity, while its average value U_0 is represented by (5.13).

$$U_0 = \frac{1}{4\pi}\int_0^{2\pi}\int_0^{\pi} U(\theta)\,\sin\theta\,d\theta\,d\varphi \tag{5.13}$$

$$= \frac{1}{4\pi}\int_0^{2\pi}\int_0^{\pi} \left[\cos\left(\frac{1}{2}\,kd\cos\theta\right)\right]^{2N-2}\sin\theta\,d\theta\,d\varphi$$

The directivity D_0 of a binomial array, based on its basic definition [27] and with no restriction in element spacing and number of elements, can be expressed as in (5.14) [as the array factor in (5.12) is only a function of θ]. For the special case of element spacing $d = \lambda/2$, (5.14) reduces to the same expression as in [27]; this is another evidence that confirms the validity of (5.14).

$$D_0 = \frac{U_{max}}{U_0} = \frac{2}{\int_0^{\pi}\left[\cos\left(\frac{1}{2}\,kd\cos\theta\right)\right]^{2N-2}\sin\theta\,d\theta} \tag{5.14}$$

By substituting $u = \frac{1}{2}\,kd\cos\theta$ and $p = 2N - 2$, (5.14) can be written as (5.14a)

$$D_0 = \frac{kd}{\int_{-kd/2}^{kd/2}[\cos u]^p\,du} \tag{5.14a}$$

It should be noted that the cosine integral in the denominator of (5.14a) can be represented in terms of a hypergeometric function $_2F_1$ [57] as in (5.14b).

$$\int \cos^p(u)\, du = -\frac{\sin(u)\cos^{p+1}(u)\, _2F_1\left(\frac{1}{2}, \frac{p+1}{2}; \frac{p+3}{2}; \cos^2(u)\right)}{(p+1)\sqrt{\sin^2(u)}} \qquad (5.14b)$$

The directivity of a binomial array with undetermined element spacing and arbitrary number of elements is achieved in (5.14). It is not simply possible to study the characteristics of the binomial array without using compact expressions for the array factor or directivity of the binomial array composed of arbitrary number of elements and undetermined spacing between the elements. In most of the designs, such as the binomial array, aim of using array antennas is to achieve high level of the directivity. It is demonstrated that binomial arrays with maximum spacing of $\lambda/2$ do not provide any side lobes [27,58]. But, the behavior of the directivity could not be simply studied or demonstrated without using (5.14).

5.4 Properties of the Binomial Array

The directivity of the binomial array can be simply demonstrated for an arbitrary number of elements and undetermined spacing between the elements using (5.14), such as in Figure 5.2. The directivity increases monotonically with increment of the element spacing up to the maximum of $\lambda/2$, in the absence of side lobes. as it is shown in Figure 5.2 for different number of elements. It's due to fact that the binomial array with maximum element spacing of $\lambda/2$ does not provide any side lobe. Subsequently, as the element spacing is increased up to $\lambda/2$, the directivity increases (Figure 5.2).
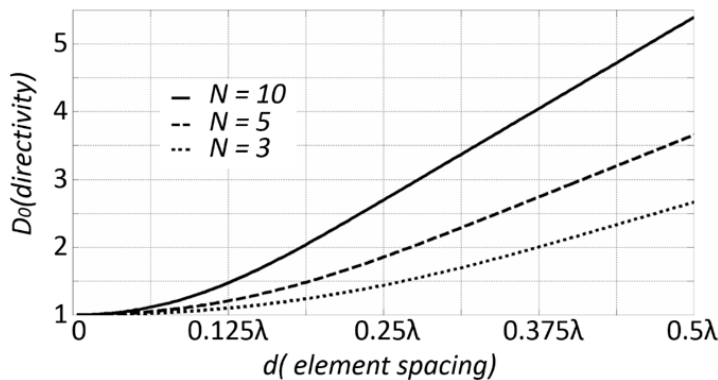
Figure 5.2 : Directivity of binomial array for different number of elements with spacing up to $\lambda/2$.

The array factor for a binomial array with different element spacing and different number of elements is shown in Figure 5.3, using (5.11).
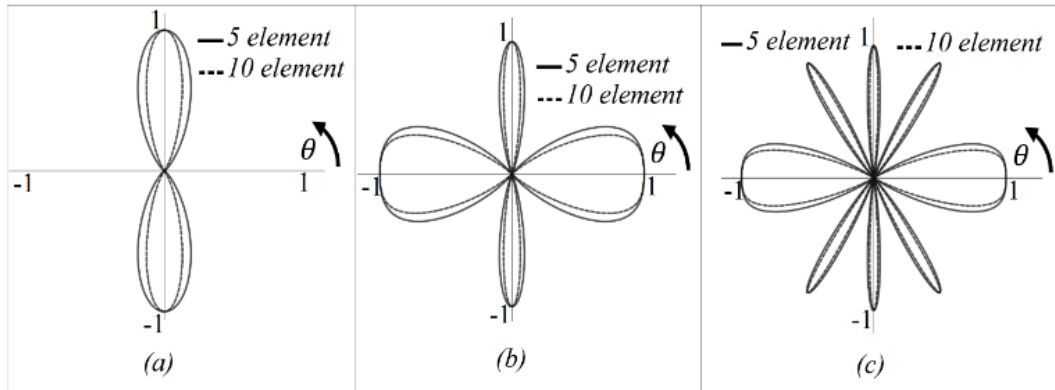
Figure 5.3 : Array factor of a binomial array for different number of elements (a) element spacing of $\lambda/2$, (b) element spacing of λ, (c) element spacing of 2λ.

It is demonstrated that for an element spacing of $\lambda/2$ there is no any side lobe. In Figure 5.2, it is shown that the directivity is increased monotonically in the absence of side lobes. However, the element spacing must be increased greater than $\lambda/2$ in order to achieve higher level of the directivity. The more the element spacing increases, the more the directivity increases. On the other hand, the more the side lobes enlarge (with element spacing larger than $\lambda/2$), the more the directivity decreases by a factor corresponding to those side lobes. Therefore, at a critical point (in spacing axis in Figure 5.4), the unwanted decrease in the directivity due to enlarged side lobes would be more than the increased directivity due to the enlarged element spacing. But, at a critical point between $\lambda/2$ and λ the directivity would be decreased due to enlarged side lobes. Consequently, determination of an optimum element spacing to achieve the maximum directivity is a critical step in the design of a binomial array. This issue is demonstrated for the arrays with different number of the elements in Figure 5.4.

It can be seen from Figure 5.4 that the critical point or optimum spacing (which gives maximum of the directivity for binomial arrays) is different for the arrays with different number of the elements. The maximum or optimum spacing for the three-element binomial array in Figure 5.4 can be considered as approximately 0.77λ which is remarkably different from the values of 0.8λ and 0.84λ observed for five-element and ten-element arrays, respectively. The line highlighted by blue color in Figure 5.4

contains the optimum values of element spacing for the arrays composed of different number of the elements.
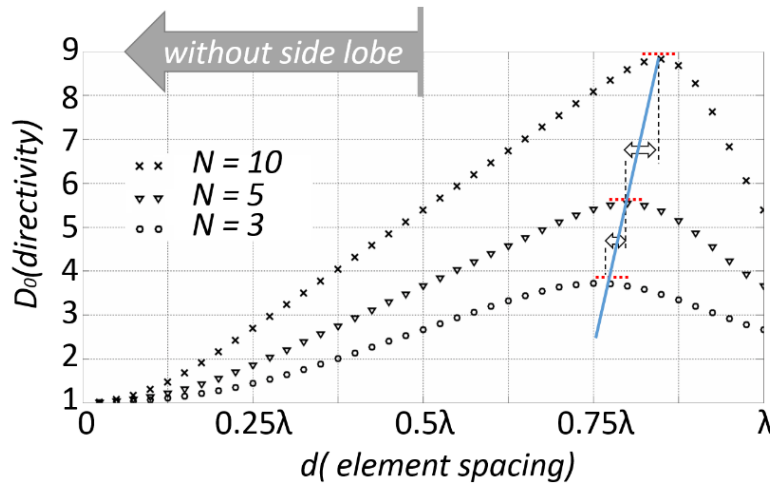
Figure 5.4 : The directivity of the binomial array for different number of elements with spacing up to λ.

It can be seen in Figure 5.3 that number of the side lobes for the arrays with a determined element spacing but containing different number of the elements is the same and limited. More precisely, number of sidelobs for binomial arrays is independent of the number of the elements in array. This property is more significant in comparison with uniformly fed arrays. Using element spacing's of λ and 2λ, only produces one and two side lobes, respectively. Therefore, this property can be considered as the additional advantage of a binomial array due to fact that the limited number of side lobes can be simply moderated or cancelled using a special element antenna.

The side lobe appeared at $\theta = 0$ degrees in the element spacing of λ (Figure 5.3) would be narrowed and shifted monotonically up to $\theta = 60$ degrees in the range of element spacing between λ and 2λ. Therefore, the greater the spacing is increased from λ to 2λ, the more the side lobes would be narrowed. Consequently, at another critical point (between λ and 2λ) the directivity begins to increase due to monotonically narrowed side lobes (shifting from $\theta = 0$ towards $\theta = 60$). But, the lobe at $\theta = 0$ degrees would appear again in a spacing between λ and 2λ as the second side lobe causing to decrease the directivity at a third critical point. These repeatedly increases and decreases of the directivity after a critical spacing's up to 4λ are demonstrated in Figure 5.5 by using (5.14).

In Figure 5.5, it can be seen that the amplitude of ripples between those critical points (maximum and minimum directivity) is regularly decreased after 4λ spacing (demonstrated by red color in Figure 5.6). for a ten-element array, tolerance between the maximum and minimum directivities (between the critical points) from λ to 4λ is decreased from $\Delta D_1 \approx 4.6$ to $\Delta D_2 \approx 1.1$.

In narrow band applications, the element spacing which gives the maximum directivity at the first critical point in the range between 0.5λ and λ may be considered as the optimum spacing. However, the directivity is suddenly decreased by increasing the element spacing from λ to 1.2λ in all the arrays with three, five and ten elements (Figure 5.5). Therefore, the element spacing around λ is not favorable for use in wide band applications. The spacing larger than λ or 2λ must be used in the wide band applications where stability of the directivity over the total band is more essential than the amount of the directivity.
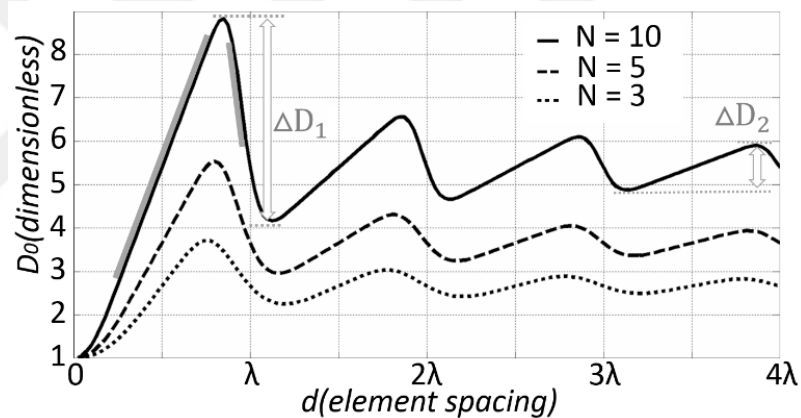
Figure 5.5 : The directivity of the binomial array for different number of elements with spacing up to 4λ.

In some applications it is required to achieve a constant directivity with stability over wide range of frequency bands. However, most of the systems, such as in amplifiers, show a linear rise or drop versus the frequency. The section of the curve in Figure 5.5 (for N=10), which is highlighted by grey color, shows the region of linear rise and drop. along with having maximum directivity. Region of the linear increase includes over 100% bandwidth for the ten-element array. Also, region of the linear decrease includes over 10% bandwidth for the ten-element array.   A uniform and constant output can be achieved over a wide band by using the binomial system having linear output with rise or drop (highlighted by blue color in Figure 5.5 for N=10), along with a system with the similar linear but inverse characteristic. Optimum number of the

elements must be determined in order to accurately adjusting slope of the directivity in inverse proportion to the slope of rise or drop in the output of the linear system. Therefore, output of the whole system can be accurately stabilized over a wide range of frequency band by selecting optimum number of the elements and optimum element spacing.

6. CONCLUSIONS AND RECOMMENDATIONS

In this thesis, novel methods of array antenna design for use in satellite communication are studied. In fact, the methods are developed based on appropriate use of array factors along with special element antennas. Three design methods are proposed to fulfill each of the three critical parameters of satellite communication (small dimensions, effective feed and narrow beam width) in Chapter 4. Validity of the proposed methods are demonstrated by theoretical calculations. However, the methods are also confirmed by simulation results and measurement (only for section 4.2) of fabricated antenna. Besides these methods, a method for calculation of the array factor and directivity of Binomial arrays, as the efficient array in terms of SLL, is presented in Chapter 5. Achieved results of all the methods are described in detail in the following.

The method in section 4.1 is proposed for array design with smaller aperture compared to the available designs. Compared results of the simulated two-element array (having $\lambda/2$ spacing) with single element antenna confirmed a 4.5dBi raise of the gain which cannot be achieved by using conventional method (λ element spacing). Then, four-element arrays with variable spacing's are simulated and compared. The results confirmed that array antennas with smaller element spacing having desired directivity can be designed. The most interesting side of the design is its simplicity, which is only based on selection of a special element antenna.

Efficiency may be considered as the most critical side of the antennas used in satellite communication. It is due to fact that high number of elements are required to be used. The method in section 4.2 describes a simple and effective method to design low loss arrays compared to complicated and high cost approaches such as waveguide feeding. The method is based on reducing the number of elements. The eight-element (with 2λ spacing) array factor based on this method is compared to the sixteen-element array factor (with λ spacing). Comparison between 3.14° and 3.15° HPBW Results achieved by 16-element and 8-element array factors, respectively confirmed the accuracy of the

method. In fact, both the array factors result in the same HPBW, where the array with 2λ element spacing includes low number of power splitters(seven) compared to the array with λ element spacing with high number of power splitters (fifteen). Also, an array is simulated and fabricated by using this method. The approximate amount of HPBW 3.2° for the simulated 8-element array confirmed that 3.15° value achieved in the calculations for the 8-element array factor. It is demonstrated that an element antenna with a very directive beam must be used to cancel the minor lobes. Then, the antennas with 4 and 8 elements are fabricated based on the proposed method. But, due to some restrictions, it was possible to measure the 4-element array antenna. Measured S11 parameter of the antenna accurately confirmed the simulated values. Finally, radiation patterns of the 4-element antenna in E-plane and H-plane are measured and desirably confirmed the simulation results. HPBW of the measured beam in E-plane reached to 5.64° that verified the simulated value of 6.2° and confirmed the ability of the antenna with a very directional beam in a single plane to be used in geosynchronous satellite applications (but number of the elements must be increased for long range satellite applications). Also, the measured beams demonstrated desirable low side lobes near to and at 30° next to the main lobe (direction of the second strong lobe in array factor with 2λ element spacing) that confirm the accuracy of the proposed method to N-element array design with 2λ element spacing with reduced number of the power splitters compared to the conventional method. However, number of the elements must be increased to achieve very lower side lobes for practical longe range satellite applications.

In section 4.3, a practical method is proposed to achieve narrower beam without increasing number of elements or dimensions of the array. A nonlinear array with optimized element spacing's is proposed and compared to linear array. Simulated results of eight-element array demonstrated at least 0.5° optimization for HPBW with acceptable level of SLL depending on the properties of element antenna. Amount of the improved HPBW is shown versus a variable range of nonlinearity. Then, the practical HPBW range for satellite communication is demonstrated, where small amount of optimized HPBW is valuable.

The studied approach and their results in Chapter 4 are advantageous to optimized different parameters of an array antenna. However, the most critical side of array antennas is their SLL which is the subject of Chapter 5 of this thesis. Binomial arrays

have been accepted as attractive array designs in terms of SLL. In this Chapter, compact expressions for the array factor and directivity of binomial arrays, with no restriction in element spacing and number of elements, have been derived and illustrated. The basic properties of Pascal's triangle and Fourier transform are used to derive them. Using these expressions, the array factor and directivity performance and the existence or absence of minor lobes, have been studied in detailed. Also, the impact of binomial array designs to stabilize the characteristics of associated communication systems, by proper selection of the optimum number of elements and associated element spacing, has been discussed.

As the future work, the proposed array configurations in this thesis will be developed. The desirable measurement results of the fabricated antenna that is designed based on Section 4.2 attracted the attention of geosynchronous satellite system. Therefore, it is aimed to develop the array antenna in a planar configuration in a way that can be fabricated in a single plane or on a single substrate layer by using an other novel method which is a combination of Broadside and Endfire array configurations. The primary simulations demonstrated very desirable results and will be developed. Furthermore, the second future work will be the design of a double-band array antenna based on the 8-element array antenna proposed in this thesis. In fact, the proposed antenna which is designed with 2λ element spacing for 11.5 GHz can be simply used also for the 8 GHz frequency band with λ element spacing with the same structure but having a different feed. Then, it will be possible to construct an effective double-band array antenna by using an effective feed network. The final recommendation and aim for the future work will be the design of an array antenna based on the Binomial method.

REFERENCES

[1] **Bevelacqua, P. J.** (2008). *Antenna Arrays: Performance Limits and Geometry Optimization*, (Ph.D. Thesis). Arizona State University, USA.

[2] **Benik, S., and Hajach, P.** (2002). Antenna Arrays-application possibility for mobile communication. *Journal of Electrical Engineering, vol. 53,* (11), pp. 332–335.

[3] **Elbert, B. R.** (2008). *Introduction to Satellite Communication*. Artech House, Inc., Third edition, Boston, London.

[4] **Gao, S., Clark, K., Unwin, M., Zackrisson, J., ….. Shiroma, W. A.** (2009). Antennas for modern small satellites. *IEEE Antennas Propag. Mag.*, *vol. 51,* (4), pp. 40–56.

[5] **Azadegan, R.** (2010). A Ku-Band Planar Antenna Array for Mobile Satellite TV Reception With Linear Polarization. *Antennas and Propagation, IEEE Transactions on, vol. 58 ,* (6), pp. 2097 – 2101.

[6] **Hall, P. S., and Hall, C. M.** (1988). Coplanar corporate feed effects in microstrip patch array design. *IEE Proceedings H - Microwaves, Antennas and Propagation, vol. 135*, pp. 180–186.

[7] **Bilgic, M.M., and Yegin, K.** (2014). Low Profile Wideband Antenna Array With Hybrid Microstrip and Waveguide Feed Network for Ku Band Satellite Reception Systems. *Antennas and Propagation, IEEE Transactions on*, *vol. 62,* (4), pp. 2258 – 2263.

[8] **Jalilfar, M., and Uddin, M. J.** (2011). Power Splitter Architectures and Applications. *PIER C, vol. 18,* pp. 231–224.

[9] **Ercoli, M., Dragomirescu, D., and Plana, R.** (2011), Small size high isolation Wilkinson power splitter for 60 GHz wireless sensor network applications. *Topical Meeting on Silicon Monolithic Integrated Circuits in RF Systems (SIRF 2011),*Phoenix, United states, pp. 85–88.

[10] **Wen, L.W., and Shen , J.Y.** (2010). A high gain array antenna with serially fed dipole elements. *Proceedings of Antennas and Propagation (EuCAP), the Fourth European Conference on*, pp. 1 – 4.

[11] **Jackson, D., and Alexoponlos, N.** (1985). Gain Enhancement Methods for Printed Circuit Antennas, *IEEE Transactions on Antennas and Propagation*, *vol. 33,* (9), pp. 976- 987.

[12] **Ando, M., Hirokawa, J., Yamamoto, T., Akiyama, A., Kimura, Y., and Goto, N.** (1998). Novel Single-Layer Waveguides for High-Efficiency Millimeter-Wave Arrays. *IEEE Trans. Microwave Theory and Techniques. vol. 46,* (6), pp. 792–799.

[13] **Zhang, Y. N., Yu, B., and Wu, D.** (2010). Low cost, high efficiency, low side-lobe array of waveguide-fed microstrip antennas. *Microw. Opt. Technol. Lett., vol. 52,* pp. 1582–1584.

[14] **Park, S. J., and Park, S. O.** (2016). LHCP and RHCP Substrate-Integrated-Waveguide Antenna Arrays for Millimeter-Wave Applications. *IEEE Antennas and Wireless Propagation Letters*, doi: 10.1109/LAWP.2016.2594081.

[15] **Tirado, J. A., Peyrot, M. A., Jardon, H., Andrade, E. A., and Reye, M.** (2006). Applications of novel defected microstrip structure (DMS) in planar passive circuits. *Proceedings of the 10th WSEAS International Conference on CIRCUITS*, July 10-12, Vouliagmeni, Athens, Greece, pp. 336–369.

[16] **Chakraborty, M., Rana, B., Sarkar, P. P., and Das, A.** (2012). Size reduction of microstrip antenna with slots and defected ground structure. *Int. J. Electron. Eng.* page:61–64.

[17] **Pandhare, R., Zade, P. L., and Abegaonkar, M. P.** (2016). Miniaturized microstrip antenna array using defected ground structure with enhanced performance. *Eng. Sci. Technol. an Int. J., vol. 19,* (3), pp. 1360-1367.

[18] **Recioui, A. and Azrar, A.** (2007). Use of genetic algorithms in linear and planar array synthesis based on Schelkunoff method. *Microw. Opt. Technol. Lett. vol. 49,* (7), pp.1619–1623.

[19] **Hussein, A. H., Abdullah, H. H. and Khamis, S.** (2012). Side Lobe Level Reduction of Linear Antenna Arrays Using a Hybrid Approach Based on MoM/GA Algorithms. *PIERS Proceedings, Kuala Lumpur, no. 1,* pp. 1328–1332.

[20] **Chartrand, M. R.** (2003). *Satellite Communications for the Nonspecialist*, SPIE Press Monograph,Washington, USA.

[21] **Harrington, R. F.** (1961). Sidelobe reduction by nonuniform element spacing. *IRE Trans. Antennas Propagat.*, pp. 187 − 192.

[22] **Dessouky, M., Sharshar, H. and Albagory, Y.** (2006). Efficient sidelobe reduction technique for small-sized concentric circular arrays. *Prog. In Electromagnetics Research, vol. 65*, pp. 187–200.

[23] **Rupcic, S., Mandric, V. and Zagar, D.** (2011). Reduction of sidelobes by nonuniform elements spacing of a spherical antenna array. *Radioengineering, vol. 20,* (1), pp. 299–306.

[24] **Tian, Y., and Qian, J.** (2005). Improve the performance of a linear array by changing the spaces among array elements in terms of genetic algorithm, *IEEE Trans. Antennas Propagat., vol. 53,* (7), pp. 2226-2230.

[25] **Sayidmarie, K. H., and Aboud, A. H.** (2008). Improvement of array radiation pattern by element position perturbation. *5th International Multi-Conference on Systems, Signals and Devices, IEEE SSD*, Jul. 20-22, doi: 10.1109/SSD.2008.4632840.

[26] **Das, S., Bhattacherjee, S., Mandal, D., and Bhattacharjee, A. K.** (2010). Optimal sidelobe reduction of symmetric linear antenna array using

genetic algorithm, *Annual IEEE India Conference (INDICON), Dec. 17-19,* doi: 10.1109/INDCON.2010.5712742.

[27] **Balanis, C. A.** (2016). *Antenna Theory: Analysis and Design,* Fourth Edition, John Wiley, Hoboken, NJ.

[28] **Stutzman, W. L., and Thiele, G. A.** (1998). *Antenna Theory and Design,* Second Edition, John Wiley & Sons, NY.

[29] **Coe, L.** (2006). *Wireless Radio: A History.* Second Ed. McFarland & Company, New York.

[30] **Alvarez, L. W.** (1989). *Adventures of a Physicist.* Basic Books, New York.

[31] **Unz, H.** (1960). Linear arrays with arbitrarily distributed elements. *IEEE Trans. Antennas Propag., vol. 8,* pp. 222-223.

[32] **King, D., Packard, R., and Thomas, R.** (1960). Unequally spaced, broad-band antenna arrays. *IEEE Trans. Antennas Propag., vol. 8*, pp. 380-384.

[33] **GODARA, L. C.** (1997). Applications of Antenna Arrays to Mobile Communications, Part 1: Performance Improvement, Feasibility and System Consideration, *Proceedings of the IEEE, vol. 85,* (7), pp. 1031-1057.

[34] **Sclub, R., Thiel, D. V., Lu, W. L., and Okeefe, S. G.** (2000). Dual- Band Six-Elements Switched Parasitic Array for Smart Antenna Cellular Communications Systems, *Electronics letters, vol. 36,* (16), pp. 1342-1343.

[35] **Ho, M. J., Stauber, G. L., Austin, M. C.** (1998). Performance of Switched-Beam Smart Antennas for Cellular Radio Systems. *IEEE Trans. on Vehic. Technology, vol. 47,* (1), pp. 10-19.

[36] **Alam, M. M., Sonchoy, M. R., Goni, M. O.** (2009). Design and Performance Analysis of Microstrip Array Antenna. *Progress In Electromagnetics Research Symposium Proceedings*, Aug. 18-21, Moscow, Russia.

[37] **Visser, H. J. (**2005). *Array and Phased Array Antenna Basics*, Wiley, July,USA.

[38] **Shahabadi, M., Busuioc, D., Borji, A., and SafaviNaeini, S.** (2005). Low-cost, high-efficiency quasi-planar array of waveguide-fed circularly polarized microstrip antennas, *IEEE Trans. Antennas Propag., vol. 53*, (6), pp. 2036–2043.

[39] **Dolph, C. L.** (1946). A current distribution for broadside arrays which optimizes the relationship between beamwidth and side-lobe level. *Proc. IRE, vol. 34,* pp. 335-348.

[40] **Harrington, R.** (1961). Sidelobe Reduction by Nonuniform Element Spacing, *IEEE Trans. Antennas and Propag., vol. 9,* pp. 187-192.

[41] **Stutzman, W. L.** (1972). Shaped-beam synthesis of nonuniformly spaced linear arrays. *IEEE Trans. Antennas Propagat.*, *vol. 20,* pp. 499-501.

[42] **Tiezzi, F., Vaccaro, S., DelRio, D. L., Grano, C. D., and Rua, M. F.** (2011). Low-profile Ku-band array antenna for broadband mobile satellite communications. *IEEE Aerosp. Conf. Proc.*, 5-12 march, pp. 1–6.

[43] **Huang, G. L., Zhou, S. G., Chio, T. H., Yeo, T. S.** (2014). Broadband and high gain waveguide-fed slot antenna array in the Ku-band, *IET Microw. Antennas Propag., vol. 8,* (13), pp. 1041–1046.

[44] **Xiang, H., and Jiang, X.** (2008). Design of a high gain microstrip antenna array at Ku-band. *2008 8th Int. Symp. Antennas, Propag. EM Theory*, 2-5 Nov., pp. 327–329.

[45] **Xianzhong, C., Yixin, Y., Qingwen, H., Xiaoli, L., Menghui, Z., Kangli, L.** (2010). A design of phased array antenna based on the Vivaldi antenna. *Industrial and Information Systems (IIS), 2nd International Conference on , vol. 1,* pp. 334 - 337.

[46] **Kimura, Y., Senga, A., Sakai, M., and Haneishi, M.** (2007). An Alternating-Phase Fed Single-Layer Slotted Waveguide Array with a Sector Shaped Beam for Millimeter-Wave Radar. *IEICE Trans. Electron., vol. E90-C,* (9), pp. 1801–1806.

[47] **Araki, K., Tanaka, A., and Matsumura, E.** (2003). Wide scanning phased array antenna design in Ka band, *IEEE Proc. Microwaves, Antennas Propag., vol. 150,* (5), pp. 379.

[48] **Recommendation ITU - R BS. 1195-1**, (2013). Transmitting antenna characteristics at VHF and UHF BS Series. *International Telecommunication Union., vol.1*.

[49] **Mokhtaari, M., and Bornemann, J.** (2008). Directional ultra-wideband antennas in planar technologies. *Proceedings of the 38th European Microwave Conference,* pp: 885–888.

[50] **Golezani, J. J., Abbak, M., and Akduman**, I. (2012). Modified directional wide band pronted monopole antenna for use in radar and microwave imaging applications, *Progress In Electromagnetics Research Letters, vol. 33,* pp. 119-129.

[51] **Xianzhong, C., Yixin, Y., Qingwen, H., Xiaoli, L., Menghui, L, Kangli L.** (2010). A design of phased array antenna based on the Vivaldi antenna, *Industrial and Information Systems (IIS), 2nd International Conference on, , vol. 1,* pp. 334 - 337.

[52] **Oppenheim, A. V., Willsky, A. S., and Nawab, H.** (1997) *Fourier analysis for continuous-time signals and systems, in Signals & systems,* second edition, NJ.

[53] **Keizer, W.** (2007). Fast low-sidelobe synthesis for large planar array antennas utilizing successive fast Fourier transforms of the array factor. *IEEE Trans. Antennas Propag., vol. 55,* (3), pp. 715–722.

[54] **Brandwood, D.** (2003). *Array Beamforming, in Fourier Transforms in Radar and Signal Processing,* 2nd Edition, Boston, London.

[55] **Ricardi, L. J.** (1972). Radiation properties of the binomial array. *Microwave J., vol. 15,* (12), pp. 20–21.

[56] **Stone, J. S.,** (1927). *United States Patent No. 1,643,323,* US patents.

[57] **Abramowitz M., and Stegun, I. A.** (1964). *Handbook of Mathematical Functions: With Formulas, Graphs, and Mathematical Tables*, National Bureau of Standards, USA.

[58] **Golezani, J. J., Paker, S., Balanis, C. A**. (2016). Compact expression for the directivity of binomial array with no restriction in element spacing, *IEEE Antennas and Wireless Propagation Letters.,* doi: 10.1109/LAWP.2016.2595107.

CURRICULUM VITAE

Name Surname:	Javad JANGI GOLEZANI
Place and Date of Birth:	Iran,Salmas - 07/02/1983
Address:	Turkey, Istanbul, İTÜ - Iran, Salmas
E-Mail:	jangi.javad@gmail.com, golezani@itu.edu.tr

EDUCATION:

- **B.Sc.**   Electronic & Communication Eng., Urmia Uni, IRAN
- **M.Sc.**   Satellite Communication & Remote Sensing,   İTÜ

PROFESSIONAL EXPERIENCE AND REWARDS:

- As a project researcher funded by two TÜBİTAK projects with grant numbers 115E225 & 113E619 working on Frequency Selective Surfaces.

PUBLICATIONS, PRESENTATIONS AND PATENTS ON THE THESIS:

- **Golezani, J. J.,** Paker S. and Balanis C. A., (2016). Compact Expression for the Directivity of Binomial Array with no Restriction in Element Spacing, *IEEE Antennas & Wireless Propagation Letters*. Doi: 10.1109/LAWP.2016.2595107.

- **Golezani, J. J.,** and Paker S., (2016). Optimization of Element Placement in Array Design for Satellite Communication, *1st International Mediterranean Sc. and Eng. Congress,* 26-28 Nov. Adana,Turkey.

OTHER PUBLICATIONS, PRESENTATIONS AND PATENTS:

- **Golezani, J. J.,** Abbak M., and Akduman, I., (2012). Modified Directional Wide Band Printed Monopole Antenna for Use in Radar and Microwave Imaging Applications, *Progress in Electromagnetics Research Letters, vol. 33*, pp. 119-129.